Fatigue and Fracture of TMI-1
Reactor Coolant Pump Shaft Failure

Prepared by

Structural Integrity Associates

Prepared for

GPU Nuclear

Prepared by: *An-Yu Kuo*   Date 10/5/84
An-Yu Kuo

Reviewed by: *[signature]*   Date 10/5/84
T. L. Gerber

Reviewed
Approved by: *[signature] P. C. Riccardella*   Date 10/5/84
P. C. Riccardella

STRUCTURAL
INTEGRITY ASSOCIATES

PREFACE

This analysis of the recent reactor coolant pump failure at Three Mile Island, Unit 1 was prepared to help achieve, along with the metallurgical failure analysis, a better understanding of the loads and failure mechanisms involved. It is intended solely as a basis for prudent planning by GPU Nuclear regarding potential mitigating measures at the TMI-1 plant, and utilizes a number of plant unique conditions and conservative assumptions. No generic implications regarding reactor coolant pump shafts in other plants are intended.

1.0 Introduction

On January 27, 1984, the vibration of a reactor coolant pump (RCP-1B) in Three Mile Island Unit-1 (TMI-1) increased from the typical 9-12 mils to 12-15 mils peak to peak. The RCP-1B vibration further increased to 19 mils and 24-28 mils peak to peak on January 30 and January 31, 1984, respectively. RCP-1B was shut down on January 31, 1984. Disassembly of the pump shaft by General Public Utilities Nuclear (GPUN) revealed the presence of an extensive circumferential crack around a thermal sleeve pin hole. The failed RCP shaft was replaced by a slightly different shaft. The failed shaft was later examined metallurgically by Babcock and Wilcox (B&W). The TMI-1 RCP-1B shaft failed at the same location and in the same failure mode as another RCP shaft failure at the Prairie Island Unit 2 plant (PI-2) three years earlier.

Structural Integrity Associates (SI) was contracted by GPUN to conduct a fatigue and fracture analysis of the failed and replacement RCP shafts. The results of the SI evaluation are documented in this report, which also includes a functional description of the pump, background information on the failure, and a summary of the B&W metallurgical evaluation for the TMI-1, RCP-1B failure.

1.1 Functional Description of Pump

Figures 1-1 to 1-4 provide a schematic illustration of the Westinghouse Model 93A Reactor Coolant Pump in use at TMI-1. There are approximately 170 Model 93A pumps in use in Pressurized Water Reactors throughout the world, of which

1-1

STRUCTURAL
INTEGRITY ASSOCIATES

70 to 80 are of essentially identical design to those at TMI-1. Basic pump characteristics are as follows:

Power = 9000 Hp Motor
Rated Flow = 88,000 GPM
Total Head = 350 feet
Speed = 1180 RPM (20 Hz)

The fluid is pumped in a radial/axial direction approximately 45° from the pump axis, by a 7 vane impeller, into a stationary 12 vane diffuser/turning vane assembly which directs the fluid to a single, radial discharge nozzle. Pump operation is essentially constant during normal plant operation, but individual pumps are often used by themself during plant startups, resulting in more severe loading than normal operation. Additionally, the pumps are sometimes jogged on and off during startups.

Table 1-1 provides a summary of the operating history of the TMI-1 pumps up to the January, 1984 shaft failure. The table provides the number of hours of single pump, cold (<350°F) operation for all four pumps. Table 1-2 presents a more detailed breakdown of single pump cold operation for the failed pump, RCP-1B, between 7/83 and 1/84. Shaft loads and stresses at the crack location for TMI-1 RCP were estimated by Westinghouse[3] and are summarized in Table 1-3.

The shaft material was procured to ASTM A-182-71 Grade F347 stainless steel with additional requirements imposed by Westinghouse. Typical properties[1] of this material are tabulated in Table 1-4.

1-2

1.2 Background Information on Westinghouse RCP Shaft Failures

A series of shaft failures[2] occurred in Model 93A pumps of an earlier shaft design in or around 1973. The most serious of these failures was at the Surry plant (in which the shaft completely severed), but subsequent examinations revealed cracking in several other shafts of the same vintage. These shaft failures occurred at a sharp groove which resulted in a very high stress concentration near the top of the thermal barrier heat exchanger (just below the pump radial bearing in Figures 1-1 & 1-2). The crack initiation site was also associated with a plug welded pin used to affix an annular thermal sleeve to the shaft at that location (see Figure 1-2). Westinghouse concluded that the rotating bending stresses due to a stationary radial thrust load on the impeller were the primary cause of the failures. Under worst case loading conditions (cold-one pump operating), this load, in conjunction with the high stress concentration and pin weld residual stresses, was just sufficient to initiate and propagate the cracking. From the comparison in Table 1-5, it is seen that the Surry pump had relatively few total operating hours at the time of failure (12,000), however, the Surry pump had the highest number of cold, single pump hours which produce the worst case loading.

In response to the "Surry-type" failures, Westinghouse redesigned[3] the 93A shaft, eliminating the upper thermal sleeve, and significantly reducing all stress concentration factors. Twelve pump shafts in operating plants were replaced, and subsequent pumps were delivered with shaft designs similar to the PI-2 & TMI-1 pump design illustrated in Figure 1-2.

1-3

In 1981, another RCP shaft failure[4] was reported in the Prairie Island, Unit 2 plant. As illustrated in Figure 1-2, the Prairie Island pump failed at the lower thermal sleeve. Once again initiation was associated with a plug welded pin used to affix the sleeve. In this case the pin weld was performed twice due to a manufacturing error. However, the calculated loads at the Prairie Island failure location were significantly less than those at the Surry location, making crack initiation and propagation more difficult to explain. Table 1-5 presents a comparison of operation times for these Surry and PI-2 failures versus that of the TMI-1 pump at the time of the recent failure. Table 1-5 also provides a comparison of radial thrust loads at the three plants. Note that although the normal operational loadings are about the same, the TMI-1 pumps see higher loads in the cold, single pump mode because of differences in plant design.

1.3 Summary of B&W Metallurgical Examination

B&W has performed a thorough metallurgical examination of the failed RCP-1B shaft. After sectioning the shaft into many pieces, a crack of 227° around the circumference and about 5" deep was found. Figure 1-5 shows a reconstruction of the failure surface showing beach marks (BM) observed in B&W's fractographic examination. The crack dimensions at these beach marks are listed in Table 1-6.

Some significant observations from the B&W failure analysis are highlighted as follows:

STRUCTURAL
INTEGRITY

(a) The fracture initiated at one side of the 0^0 pin hole and rapidly enveloped the entire pin hole.

(b) A well preserved beach mark pattern was observed.

(c) Crack growth eventually became non-symmetric with the most rapid crack growth against the direction of shaft rotation.

(d) The area containing the vast majority of beach marks (up to BM #15) was also the area of highest corrosion deposit, exhibiting a distinct red-brown color.

(e) The BM #15 contained one array of large pits which followed the beach mark. This was the only location in the entire fracture surface which had any pitting.

(f) The fractography over the initial 1" (i.e. up to BM #15) of depth indicates a low ductility, transgranular crystallographic fracture mode.

(g) Striations were found from BM #15 to the final crack position (about 1" to 5"). The striations were 0.2, 0.1 to 0.2, and 0.3 microns (1 micron = 7.9×10^{-6} inch) in spacing over the fracture surface of 1" to 2.5", 2.5" to 3", and 3" to 5", respectively.

(h) Most of the fracture was a fine transgranular structure with crack propagation occurring on many planes or plateaus, although small amounts of intergranular and/or cleavage facets exist from 2.5" to 5".

STRUCTURAL
INTEGRITY ASSOCIATES

(i) The crack extends about 227° around the shaft circumference and has an axial component of 0.75" over the 227°.

(j) No cracking has been observed in the 180° pin hole.

(k) Although sulphur was found on the fracture surface, there was no evidence to suggest that its presence had initiated the cracks and/or accelerated crack growth. No other deleterious species, such as Cl, was found and the shaft material chemistry was within specification.

TABLE 1-1

TMI-1 RCP Operating History
(Cold, Single Pump)

Time	Hours			
	A	B	C	D
4/75 - 5/78*	10	6	1/2	1
7/83 - 1/84	0	1363	1212	0

* Preliminary Information

TABLE 1-2

TMI-1 RCP-1B Operating History
(Cold, Single Pump)

From	To	Hours
7/2/83	7/4/83	48
7/4/83	7/8/83	82
7/9/83	7/11/83	48
7/13/83	7/15/83	48
7/17/83	7/19/83	48
7/21/83	7/23/83	48
8/1/83	8/2/83	20
8/23/83	8/27/83	96
10/25/83	12/9/83	245
12/20/83	12/27/83	180.5
1/5/84	1/12/84	169.5
1/17/84	1/31/84	330

STRUCTURAL
INTEGRITY

TABLE 1-3

Shaft Loads and Stresses* at Crack Location
For TMI-1 RCP

	One Pump - Cold Operation	Hot Operation
Motor Torque	2904	2691
Axial Thrust	826 (49690)	943 (56690)
Radial Thrust	+ 2836 (10,000)	+ 1347 (4750)
Cyclic Torque	+ 87	+ 81
Cyclic Axial Load	N/A	N/A
Rotating Radial Load	285 (635)	215 (480)

* First number in PSI; number in parenthesis is load in LBS or IN-LBS.

TABLE 1-4

Material Properties of F347 Stainless Steel

0.2% Yield Strength	33.5 - 37 ksi
Ultimate Tensile Strength	77.5 - 83.5 ksi
Elongation in 2"	53.5 - 58%
Reduction in Area	67 - 70.5%

STRUCTURAL
INTEGRITY

TABLE 1-5

Summary of Failures at Other Plants

	Surrey	PI-2	TMI-1
"Cold" Hours (Single Pump)	1642	581	1,360
"Hot" Hours	9649	51,573	35,000
Failure Location	Upper Sleeve*	Lower Sleeve	Lower Sleeve
Failure Mode	Rotating Bending	Rotating Bending	Rotating Bending
Crack Initiation	Severe Local Stress at Groove	Localized High Residual Stress Due to Pin Welding	Localized High Residual Stress Due to Pin Welding

* not used on PI-2 and TMI-1

Radial Thrust Loads:			
Normal Operation	-	3,605 lbs	4,750 lbs
Cold, Single Pump	7,700	5,140 lbs	10,000 lbs

STRUCTURAL
INTEGRITY ASSOCIATES

TABLE 1-6

BEACH MARK LOCATIONS[1]

Beach Mark No.	Left Circumferential (Intercept)[2]	Left Vector Intercept[3]	Intercept[3]	Right Vector Intercept[3]	Right Light Circumferential Intercept[4]
1	-----	-----	-----	0.068	0.286, 3.75°
2	-----	-----	-----	0.300	0.509, 6.67°
3	-----	-----	-----	0.426	0.653, 8.55°
4	-----	-----	0.611	-----	-----
5	0.572, 7.49°	0.561	-----	-----	-----
6	0.675, 8.84°	0.636	-----	-----	-----
7	0.771, 10.10°	0.691	-----	-----	-----
8	0.827, 10.83°	0.737	-----	-----	-----
9	0.937, 12.27°	0.801	0.721	0.651	0.954, 12.49°
10	0.970, 12.70°	0.836	0.742	0.674	0.970, 12.70°
11	1.462, 19.15°	-----	-----	-----	-----
12	1.543, 20.21°	-----	-----	-----	-----
13	1.653, 20.65°	1.251	-----	-----	-----
14	1.685, 22.07°	1.302	0.884	0.869	1.288, 16.87°
15	1.749. 22.95°	1.372	0.907	0.894	1.370, 17.29°
16	-----	1.476	0.936	0.956	1.375, 18.01°
17	-----	1.543	-----	-----	1.415, 18.53°
18	-----	1.768	-----	1.024	-----
19	-----	-----	-----	1.084	-----
20	-----	-----	-----	1.272	-----
21	-----	-----	-----	1.812	-----
22	-----	-----	-----	2.162	-----
23	-----	-----	-----	2.797	-----
24	-----	-----	-----	3.258	-----
25	-----	-----	-----	4.784	-----
26	-----	-----	-----	-----	-----
27	-----	-----	-----	-----	-----
28	-----	-----	-----	-----	-----
29	-----	-----	-----	-----	-----

Notes:

[1] See Figure 1-5

[2] First number is arc length (in) from ₵ of pin hole to beach mark intercept at surface; second number is angle subtended by the measured arc length.

[3] Distance from LV, ₵ , or RV vector origin to beach mark intercept. Units are inches.

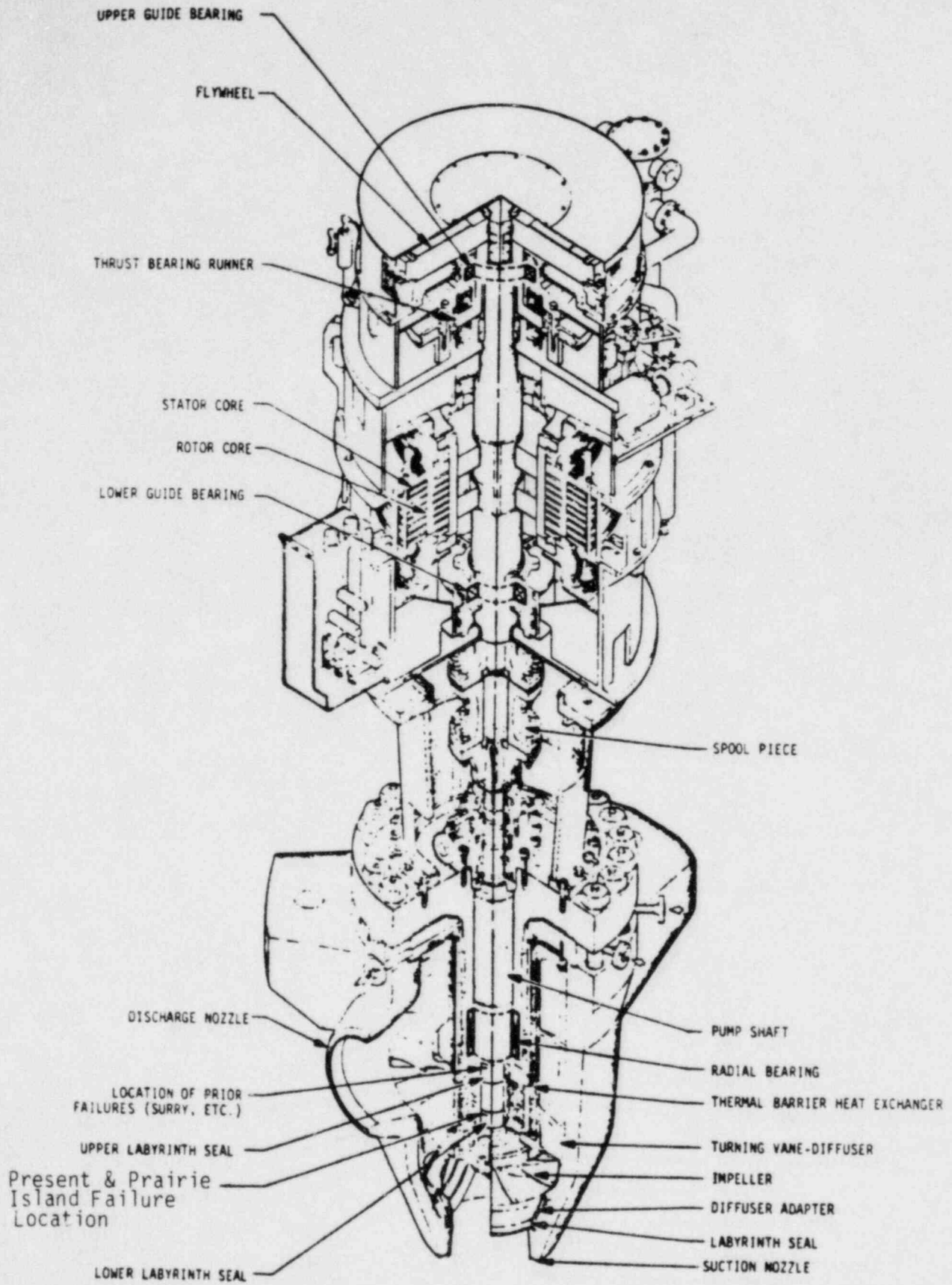[4] Same as 2 except arc length measured from crack initiation at right side of hole mosaic.

UPPER GUIDE BEARING

FLYWHEEL

THRUST BEARING RUNNER

STATOR CORE

ROTOR CORE

LOWER GUIDE BEARING

SPOOL PIECE

DISCHARGE NOZZLE

PUMP SHAFT

RADIAL BEARING

LOCATION OF PRIOR
FAILURES (SURRY, ETC.)

THERMAL BARRIER HEAT EXCHANGER

UPPER LABYRINTH SEAL

TURNING VANE-DIFFUSER

Present & Prairie
Island Failure
Location

IMPELLER

DIFFUSER ADAPTER

LABYRINTH SEAL

SUCTION NOZZLE

LOWER LABYRINTH SEAL

Figure 1-1   Schematic Illustration of Model 93A Pump

1-11

Bearing
(.017 - .021 Dia.)

Crack Location; SURRY
(Location 2)
at Pin Hole Under Sleeve
(No Sleeve Shown)

Upper T.B. Labyrinth
(.020 - .028 Dia.)

Crack Location. T M I - 1, P1-2
(Location 1)

Lower T.B. Labyrinth
(.020 - .028 Dia.)

Upper Impeller Labyrinth
(0.050 on Radius
.100 on Diameter)

Lower Impeller Labyrinth
(0.050 on Radius
.100 on Diameter)
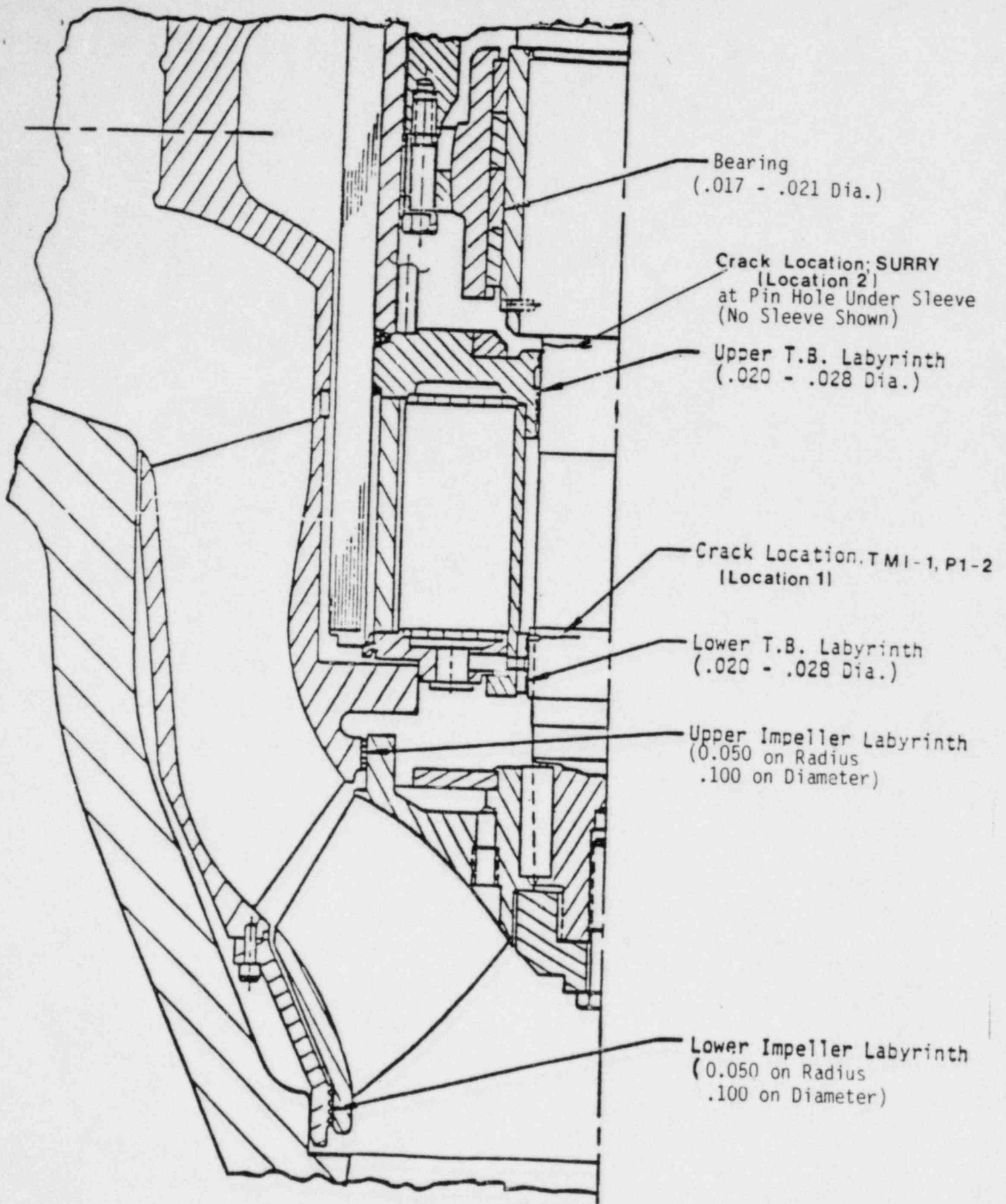
Figure 1-2   Failure Location Details

STRUCTURAL
INTEGRITY ASSOCIATES
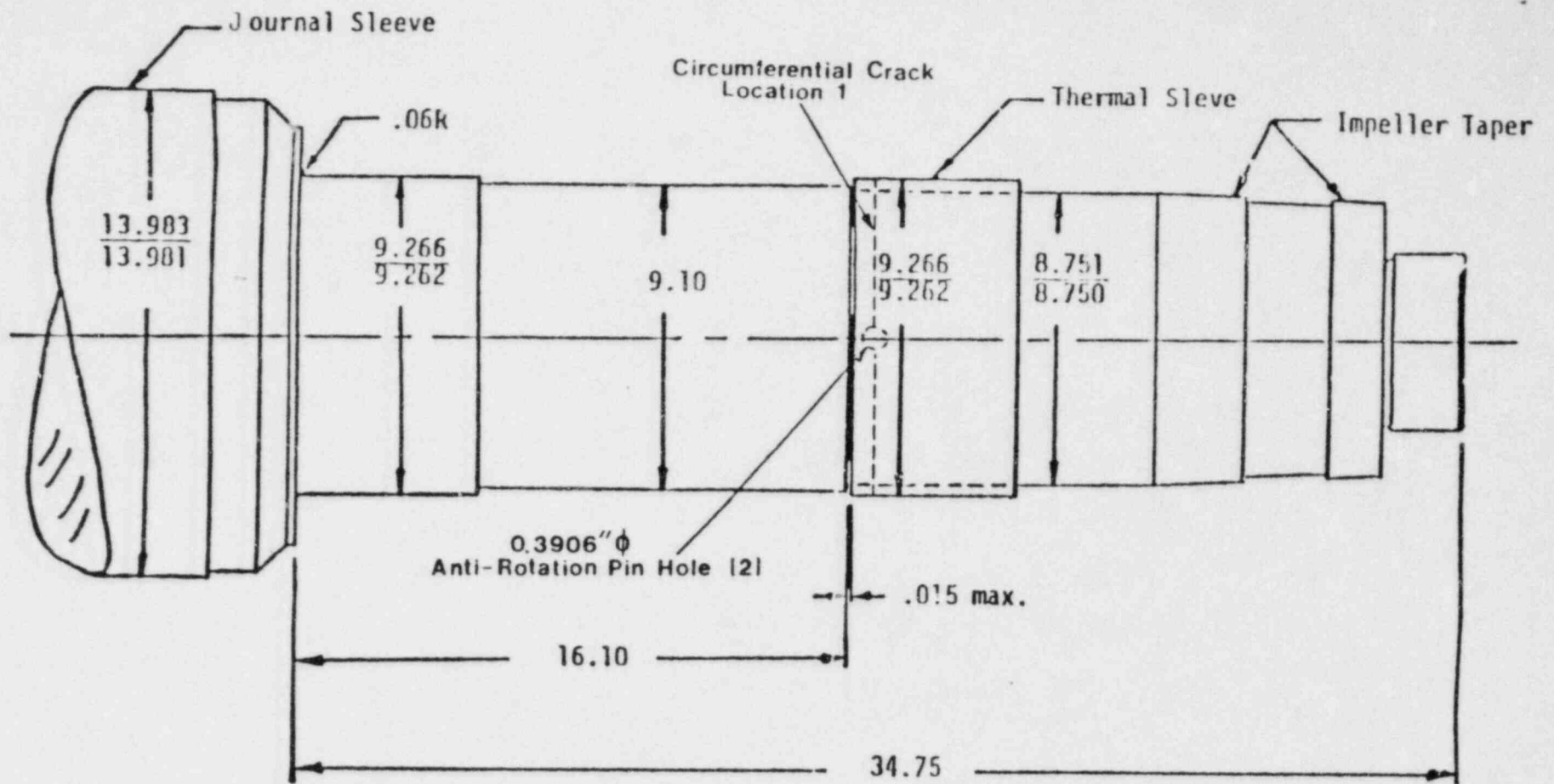
TYPE B SHAFT

Figure 1-3   Shaft Dimension
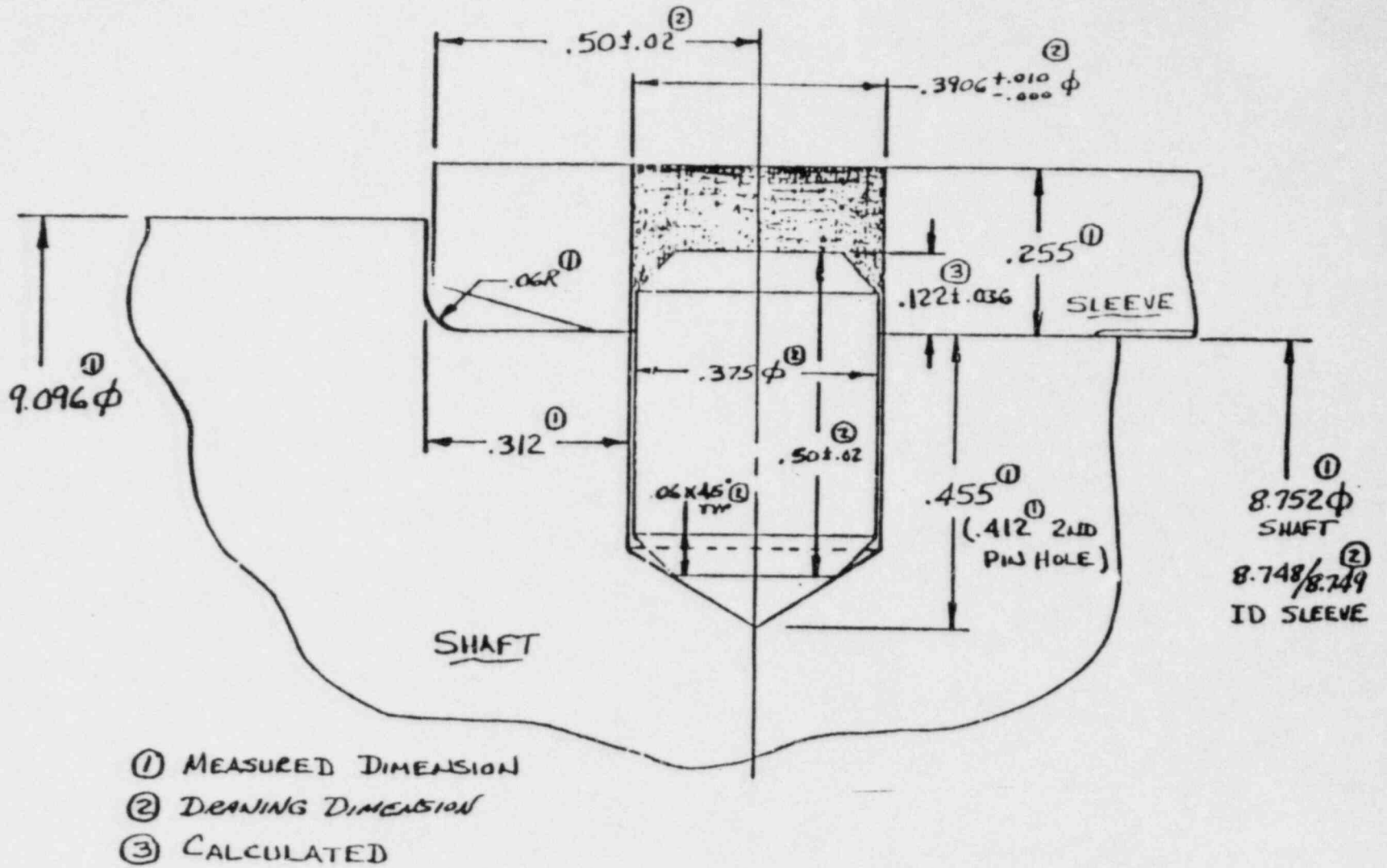
Figure 1-4   Pin and Pin Hole

① MEASURED DIMENSION
② DRAWING DIMENSION
③ CALCULATED
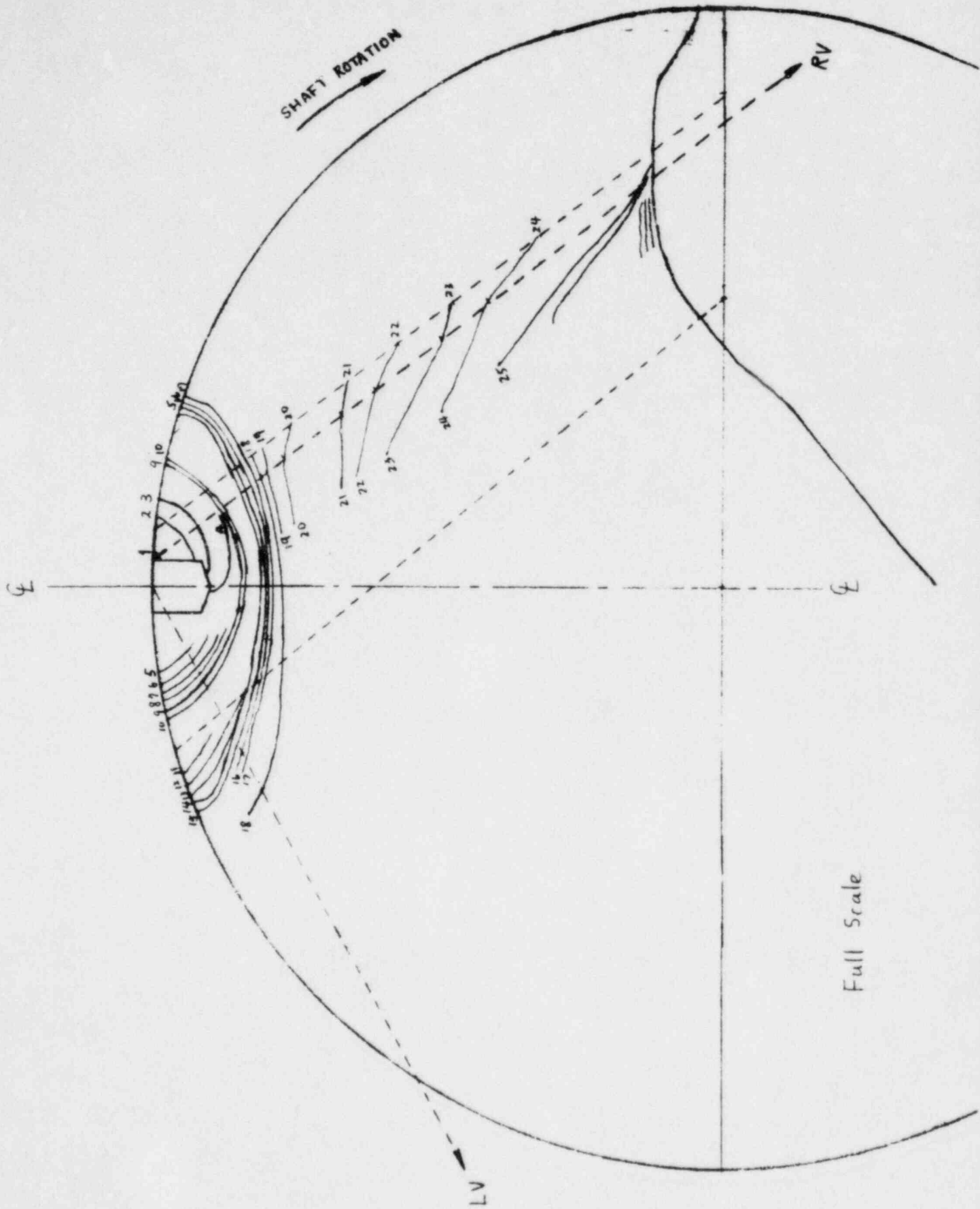
Figure 1-5   Reconstructed Beach Marks

1-15

2.0 Fatigue and Fracture Analysis

2.1 Stress Intensity Factor Calculations

In order to carry out the fracture/fatigue analysis of the RCP shaft, an accurate calculation of stress intensity factor is necessary. Since, the bending due to the radial thrust load is believed to be the major cause of the shaft failures, only the stress intensity factors resulting from this loading are discussed here. Other loads, such as axial thrust and torsion were addressed by Westinghouse in prior reports[2,3,4] but are not believed to have played a major role in the failures.

The stress intensity factor for a single-edge-cracked round shaft under bending loading can be expressed as[5]

$$K = Y' M/D^{2.5} \qquad (1)$$

where D is the shaft diameter, M is the applied bending moment, and Y' is a function of the ratio of crack depth to shaft diameter (a/D). Y' has been determined experimentally[5]. Figure 2-1 shows the values of Y' at various crack depths (a/D). In Reference 5, compliance of the shaft at different crack depths has also been measured. Converting the compliance into stiffness, two sets of shaft stiffnesses corresponding to two different shaft length to diameter ratios, S/D, are shown in Figure 2-2. Calculations based on beam theory are also plotted in Figure 2-2 for comparison. The (S/D) ratio of the IMI-1 RCP shaft (S/D = 2 × 18.65/8.75 = 4.26) is between those of the two measurements (3.33 and 6.69) reported in Reference 5. A best

2-1

estimate curve is drawn in Figure 2-2 to represent the bending stiffness reduction of a cracked RCP shaft.

Equation (1) gives the stress intensity factors of a cracked shaft under constant load, i.e., P remains constant in Figure 2-2. If instead of constant load, a constant displacement condition at the loading point is imposed, i.e., P decreases as the crack grows deeper in Figure 2-2, the stress intensity factors should be calculated by

$$K = Y' M \ (I/I_0)/D^{2.5} \tag{2}$$

where (I/I_0) is given in Figure 2-2, and all the other parameters are defined the same as in Equation (1). Figure 2-3 shows the stress intensity factors under constant load of 10,000 lbs and a constant displacement equal to that corresponding to 10,000 lbs load in the uncracked shaft. It is seen that as the crack grows deeper than 20% of shaft diameter, the stress intensity factors under constant load increase substantially, whereas the stress intensity factors under constant displacement stay almost constant up to 60% of shaft diameter. It should be noted that the displacement resulting from 10,000 lbs radial thrust is not the same as the displacement restraint imposed by the clearance between the impeller and the labyrinth seals (see Figure 1-2, ~0.050 inch radial clearance for TMI-1 RCP). Based on a finite element analysis which will be explained in detail in Section 2.2, 10,000 lbs radial thrust at the impeller will cause a deflection of 0.080 inches, which is greater than the clearance.

STRUCTURAL
INTEGRITY

Another factor which needs to be considered in the stress intensity factor calculation is the potential for dynamic amplification of the applied load. As will be discussed in Section 2.2, a dynamic amplification factor (DAF) of approximately 2 can be expected for the TMI-1 RCP shaft at 1180 rpm. Therefore, the amplitude of stress intensity factor variation, ΔK, for the RCP shafts can be written as

$$\Delta K \simeq 2 \cdot (DAF) \cdot K = 4 \cdot K \qquad (3)$$

where K is calculated by Equation (1) or (2).

After considering the clearance restraint of the labyrinth seals and the dynamic amplification, the ΔKs for a cracked RCP shaft under single pump and normal operation have been calculated and are plotted in Figure 2-4. In Figure 2-4, the single pump curve is derived assuming a constant displacement condition, whereas the normal operation curve is derived from a constant load condition up to 3.3 inch crack depth, and a constant displacement afterwards.

2.2 Dynamic Amplification Model

Figure 2-5 illustrates a dynamic finite element model developed by SI personnel during a prior failure analysis performed of the PI-2 pump shaft[4]. The shaft is modeled as a continuous beam with variable cross-sectional area properties according to the shaft physical dimensions. The model is believed to be equally applicable to the TMI-1 pumps. As shown in Figure 2-5, the thrust bearing, upper and lower motor bearings and pump bearings are all represented as linear springs with spring constants on the

2-3

order of 10^6 lbs/in (this value was provided by Westinghouse). The flywheel, impeller, and rotor are modeled as lump masses. The static deflection and mode shapes of the RCP structure were calculated using the computer code STARDYNE[6]. Only the bending mode, which has been identified as the principle fracture mode for both the PI-2 and TMI-1 RCP shafts, was addressed by the model.

From the static analysis, an impeller deflection of 0.00813 inches was calculated for a 1,000 lbs radial thrust force applied at the impeller, i.e., 8.13×10^{-6} in/lb. Thus, under single pump operation, the 10,000 lbs radial thrust would close the radial clearance of 0.050 inches between the impeller and labyrinth seal. This 0.050 inch gap is not expected to be closed when the RCP is under normal operation (4750 lbs axial thrust). Note also that the gap on one side of the pump could be somewhat greater than 0.050 inches (but less than 0.100 inches) due to initial offset of the impeller. 0.060 inches has been used in the analyses which follow. The natural frequencies of the first four bending modes of the shaft are 26.3, 27.26, 31.98 and 50.84 Hz, respectively. Their corresponding mode shapes are shown in Figures 2-6 through 2-9, respectively. It is seen that the operating frequency (20 Hz) is close to those of the first two bending modes.

The next task in the dynamic analysis of the RCP shaft was to estimate the dynamic amplification factor. By applying a constant amplitude, sinusoidal radial force or displacement at the impeller (Node 1 in Figure 2-5), the dynamic amplification at the location of the TMI-1 and PI-2 failures can be determined. Dynamic amplification factors (DAF) at several frequencies have been calculated. Results of these DAF calculations are illustrated in Figure

STRUCTURAL
INTEGRITY

2-10. Both undamped and 2% damping (which is generally considered to be a reasonable value in mechanical components) have been analyzed. It is seen from Figure 2-10 that DAFs at the crack location equal to 3.1 and 2.0 are predicted for the undamped and 2% damping cases, respectively. A DAF = 2.0, has been used in the balance of this study.

2.3 Material da/dN and Striation Curves

Research into available literature by SI produced a paper by Bathius and Pelloux[7] which correlates macroscopic growth rate and striation spacing with K for austenitic stainless steels similar to the TMI-1 pump shaft. Data from this paper, presented in Figure 2-11, show that under the laboratory conditions tested (room temperature, air, 10 Hz), striation spacing exceeded the measured crack growth rate by nearly two orders magnitude at low K levels. This means that the actual rate of advance of the crack front was probably considerably less than that indicated by the striation spacing. Pelloux attributed this behavior to localized advance of the crack front. That is, the crack advances along a very small portion of the crack front while the remainder of the crack front remains dormant. Material crack growth curves given by Bathius and Pelloux[7] for austenitic stainless steel also agree well with empirical equations given by Bates and Clark[8] for a large group of materials.

In this report, the curves given by Bathius and Pelloux are used in the fatigue/fracture evaluation of the TMI pump shaft. The two curves may be written explicitly as

$$da/dN = 8.74 \times 10^{-15} (\Delta K)^{5.66} \qquad (4)$$

for macroscopic crack growth, and

$$da/dN = 3.25 \times 10^{-8} (\Delta K)^{1.84} \qquad (5)$$

for striation spacing where the units for da/dN and ΔK are in./cycle and ksi $\sqrt{in}$, respectively.

2.4 Correlation of Beach Marks and Operational History

Based on the B&W fractography and SI's calculations described in Sections 2.1 to 2.3, SI is able to postulate a plausible fatigue crack propagation mechanism for the TMI-1 RCP shaft:

(i)   The applied ΔK must be greater than $(\Delta K)_{threshold}$ (5 ksi $\sqrt{in}$) to propagate the crack.

(ii)   The failure was primarily a rotational bending fatigue fracture, with a small amount of torsional contribution to the crack propagation, and little or no stress corrosion or corrosion assist.

(iii)   Beach mark #15 was the crack front at the time of the 1979 shut down, as well as at the beginning of the 1983 lay-up period.

STRUCTURAL
INTEGRITY

(iv) A combination of near yield level residual stresses due to pin welding and about 10 hours of single pump operation were needed to initiate a crack of $a_0 \approx 0.5$ inches, which is the minimum crack depth required to reach (ΔK)threshold under normal operating loads.

The first hypothesis is a reasonable assumption for typical 347 stainless steel. From Figure 2-4, it is seen that the crack has to be deeper than .2 inches and .5 inches, respectively, under single and multiple pump operating loads to achieve the 5 ksi $\sqrt{in}$. threshold.

The second hypothesis is strongly supported by the resemblance of the TMI-1 RCP-1B fracture surface to a typical "textbook" example[9] of unidirectional, rotating bending with low stress and a low stress concentration as illustrated in Figure 2-12. Hypothesis (iii) is based mainly on the B&W metallurgical examination results especially (d), (e) and (h) in Section 1.3. The last hypothesis is drawn from SI's best judgement; however, in the later part of this section, SI will show some verification for this hypothesis.

To further check the above hypothesis, SI examined the correlation between the beach marks and operational history by employing the stress intensity factor calculation, dynamic amplification factors, and material da/dN curves mentioned in the previous sections.

STRUCTURAL
INTEGRITY

2.4.1 After BM #15

Crack propagation from BM #15 to the final crack front, i.e., a = 1.4 inches to 5.3 inches in Figure 2-4, involved 1363 hours of single pump operation according to the operational history for RCP-1B listed in Tables 1-1 and 1-2. SI's fatigue crack growth analysis predicts 1350 hours of single pump operation. This good agreement confirms the adequacy of SI's ΔK calculation and da/dN curves. In addition, the striation spacing of 0.14 microns predicted by using Figures 2-4 and 2-11 falls in the range of 0.1 to 0.3 microns reported by B&W.

The crack front locations predicted by SI's fatigue crack growth analysis are compared with the beachmarks measured by B&W and the RCP-1B single pump operation 1 history during the 1983 lay up in Table 2-1. There is a very good correspondence between the beach marks and the operational record for BM #15 and BM #21 to BM #25.

Due to the shorter operating hours between 7-2-83 and 8-27-83, the correlation between beach marks and number of startups is less precise in this region. The other three beach marks, BM #16, 17, and 18, fall in this period but their correlations with the 7 pump startups may be slightly different from those shown in Table 2-1.

From the correlation given by Table 2-1, it is interesting to note that the vibration monitor was not able to pick up the RCP shaft cracking until the crack reached approximately 3.4 inches in depth. From SI's fatigue crack growth analysis, the hours required to grow a crack from 0.3 inches to 0.4

STRUCTURAL
INTEGRITY

inches, 0.4 inches to 0.5 inches, 0.5 inches to 1.4 inches, and 1.4 inches to 5.5 inches are illustrated in Figure 2-13. Using this figure, and the four hypotheses mentioned above, and assuming 35,000* hours of multiple pump operation through the 1979 shut down, postuled crack depths for the four pumps at the 1979 shutdown and of the end of 1983 operation are tabulated in Table 2-2. According to this table, only pump B would have had cracks greater than 3.4 inches crack size, the other three pumps still being far from a detectable failure. This result provides a plausible explanation of why failure was only observed in RCP-1B when both RCP-1B and RCP-1C experienced about the same number of hours of single pump operation after the 1979 shutdown. Please note that there are some intentional conservatisms in the calculations leading to Table 2-2. The crack depth estimates may thus be somewhat overstated, and are presented in this manner mainly to provide a prudent basis for future planning.

2.4.2 Before BM #15

Figure 2-14 presents a crack initiation hypothesis, in which, as a result of welding residual stresses and stress concentration, many micro-cracks initiate around the pin hole. These small cracks could be corner cracks as shown in Figure 2-14(c) or semi-circular surface cracks as shown in Figure 2-14(d). When the ΔK at these crack fronts become greater than the threshold

---

* This assumption implies that the pre-1979 operation occurred in a worst case manner, in which the cold-operational hours for each pump were accumulated first, followed by 35,000 hours of single pump operation. More likely operating patterns would suggest the cold operation to be evenly distributed with the 35,000 hours, resulting in less severe crack growth.

ΔK value, (≈5 ksi √in.), these micro-cracks would grow, coalesce, and form an equivalent semi-circular surface crack of about 0.5 inches deep as shown by the dashed line in Figure 2-14(a). This semi-circular surface crack can be modeled as an edge crack in a round shaft as illustrated in Figure 2-14(b), since up to 0.5 inches in crack depth, the stress intensity factor for a semi-circular crack in a half-space is approximately the same as that of an edge crack in a shaft (Figure 2-4).

Although it is difficult to determine the exact residual stress distribution due to the pin welding, as also pointed out in Reference 4, the magnitude of the residual stress might have been as high as 60 to 70 ksi. As a conservative bench mark, SI has assumed a residual stress distribution as illustrated in Figure 2-15. In Figure 2-15, the horizontal axis, r, stands for the distance measured from the shaft or pin hole surface.

Even though the residual stress doesn't change the ΔK, it can create high, positive R-ratios for cracks of 0.2 inches or shallower, where R-ratio is defined as the ratio of the maximum and minimum K values in the cyclic loading. The high R-ratio will change the fatigue crack propagation speed. Generally, R-ratio effects are taken into consideration in crack growth analyses by replacing the ΔK in equation (4) with $(\Delta K)_{eff}$ where

$$\Delta K_{eff} = \frac{\Delta K}{(1-R)^{0.5}}$$

An estimate of R-ratio effects due to residual stresses is depicted in Figure 2-16. In this figure, the solid curves and dashed curves are ΔK_{eff} curves

STRUCTURAL
INTEGRITY

before and after the R-ratio correction, respectively. It is found that the R-ratio effects become insignificant beyond a crack depth of 0.2 inches. Curves are provided in Figure 2-16 for both single pump and normal (multi-pump) operation.

As discussed earlier in this report, the RCP shaft material is estimated to have a threshold ΔK value of ~5 ksi $\sqrt{in}$. for fatigue crack growth. From Figure 2-16, it is seen that the minimum semi-circular surface crack sizes to achieve $(\Delta K)_{th}$ are .035 inches and 0.45 inches under single pump and multiple pump loading conditions, respectively. By the same procedure, the critical crack sizes can be calculated for a corner crack in a quarter-space. Table 2-3 tabulates the minimum crack sizes to achieve $(\Delta K)_{th}$ for two crack models under two loading conditions.

It is seen that the critical crack sizes under multiple pump loading conditions are an order of magnitude greater than those under single pump loading condition. Thus, the micro-cracks around the pin hole were far more likely to grow and coalesce into a 0.5 inch edge crack in the RCP shaft under single pump operation than those under multiple pump operation. This provides one rationale for the hypothesis (iv) in Section 2.4.

2.5 Fatigue Initiation Analysis

2.5.1 Original Shafts

Figure 2-17 presents a crack initiation curve for the 347 SS pump shaft material provided by Westinghouse in Reference 3. The effect of mean stress

is accounted for in this curve through the use of a standard Goodman/-Soderberg diagram as illustrated in Figure 2-18. Such a diagram provides an approximate means of accounting for the interaction of mean and alternating stress in high cycle fatigue. A straight line is constructed between the critical alternating stress of the appropriate number of cycles, and a mean stress equal to the material ultimate tensile strength. The critical alternating stress at any mean stress is then given by this straight line. A second fatigue curve adjusted for an assumed 60 ksi residual stress due to the pin welding operation is thus plotted in Figure 2-17, using the Goodman/Soderberg methodology. From this curve, it is seen that the RCP shaft under single pump operation (4.2 ksi = 2 x 2.8 x 0.06/0.08) would require operation for 10^6 cycles (14 hours at 1180 rpm) to initiate small cracks, but that no cracking would be expected to initiate under multiple pump operation (2.8 ksi = 2 x 1.4). This result provides a further rationale for the 10 hour assumption in hypothesis (iv) as well as the whole statement of hypothesis (iv).

2.5.2 Replacement Shafts

The replacement shaft installed by GPU in RCP-1B has essentially the same dimensions but a more generous shoulder radius. (3/8 inches instead of 0.06 inches) in Figure 1-4, as the failed shaft. This 3/8 inch radius would substantially reduce the stress concentration factor at the shoulder, however, as shown in Figure 1-4, the shoulder is 0.312 inches away from the pin weld. The residual stress effects due to the pin welding are expected to die out at a distance of 0.2 inches from the weld. Thus, the shoulder radius

STRUCTURAL
INTEGRITY

change is not believed to provide a significant improvement over the original

shafts from the standpoint of fatigue crack initiation and propagation from

the thermal sleeve pin hole.

STRUCTURAL
INTEGRITY

TABLE 2-1

ΔT (hrs)	SI Calculation			B&W Measurement		Operating Records
	T (hrs)	a* (in.)	a_{RV}^* (in.)	BM	a_{RV}^* (in.)	
	0	1.39	.89	# 15	.894 ± .15	
50 ➤						◄— 7-2-83 to 7-4-83, 48 hrs
	50	1.46	.96			
80 ➤						◄— 7-4-83 to 7-8-83, 82 hrs
	130	1.57	1.07	# 16	.956 ± .15	
50 ➤						◄— 7-9-83 to 7-11-83, 48 hrs
	180	.164	1.14			
45 ➤						◄— 7-13-83 to 7-15-83, 48 hrs
	225	1.71	1.21	# 18	1.024 ± .25	
50 ➤						◄— 7-17-83 to 7-19-83, 48 hrs
	275	1.79	1.29			
45 ➤						◄— 7-21-83 to 7-23-83, 48 hrs
	320	1.88	1.38	# 19	1.292 ± .30	
20 ➤						◄— 8-1-83 to 8-2-83, 20 hrs
	340	1.91	(.4)			
100 ➤						◄— 8-23-83 to 8-27-83, 96 hrs
	440	2.12	1.62	# 21	1.812 ± .35	
240 ➤						◄— 10-25-83 to 12-9-83, 245 hrs
	680	2.74	2.24	# 22	2.162 ± .5	
180 ➤						◄— 12-20-83 to 12-27-83, 180 hrs
	860	3.35	2.85	# 23	2.797 ± .7	
170 ➤						◄— 1-5-84 to 1-12-84, 170 hrs
	1030	4.09	3.59	# 24	3.258 ± .7	
330 ➤						◄— 1-17-84 to 1-31-84, 330 hrs
	1360	5.45	4.95	# 25	$4.734 \pm \begin{smallmatrix}0.\\1.\end{smallmatrix}$	

1363 hrs.

* See Figure 2-4, a = a_{RV} + 0.5"

2-14

STRUCTURAL INTEGRITY

TABLE 2-2

Postulated Crack Depths for the Four TMI-1 Pumps
Under SI's Failure Hypothesis

Pump	Crack Depth at 1979 Shutdown	Crack Depth at End of 1983 Operation
RCP-1A	1.4 inches	1.4 inches
RCP-1B	1.4 inches	5.5 inches
RCP-1C	0.0 inches	0.6 inches
RCP-1D	0.0 inches	0.0 inches

Table 2-3

Minimum Crack Depth Required
To Achieve $\Delta K = 5$ ksi $\sqrt{\text{in}}$

Loading		
Residual Stress + Single Pump	0.035 inches	0.025 inches
Residual Stress + Multiple Pump	0.45 inches	0.45 inches

STRUCTURAL INTEGRITY
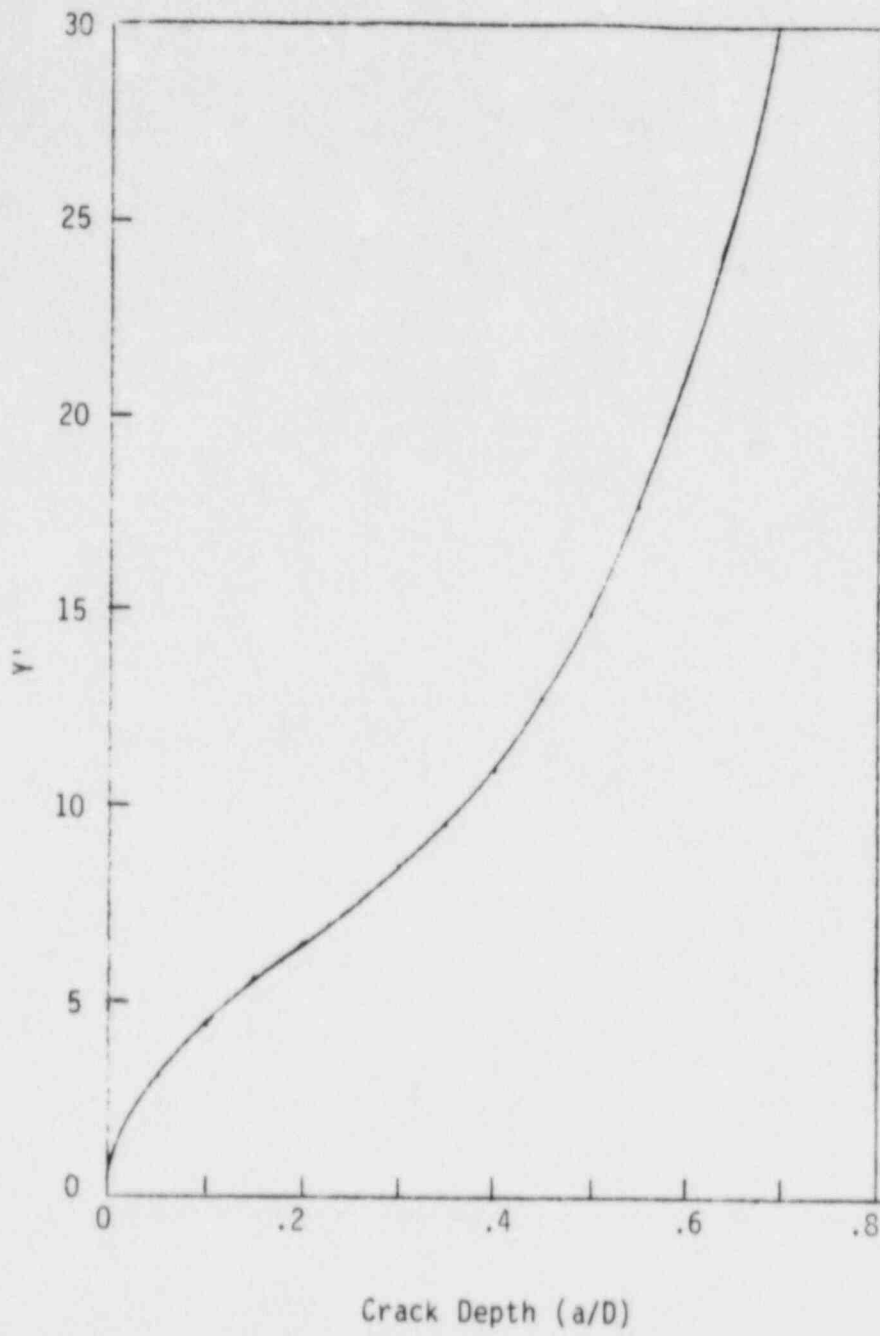
Figure 2-1 Y' For Crack Shafts

STRUCTURAL
INTEGRITY

Figure 2-2 Bending Stiffness Change Due To Crack Growth
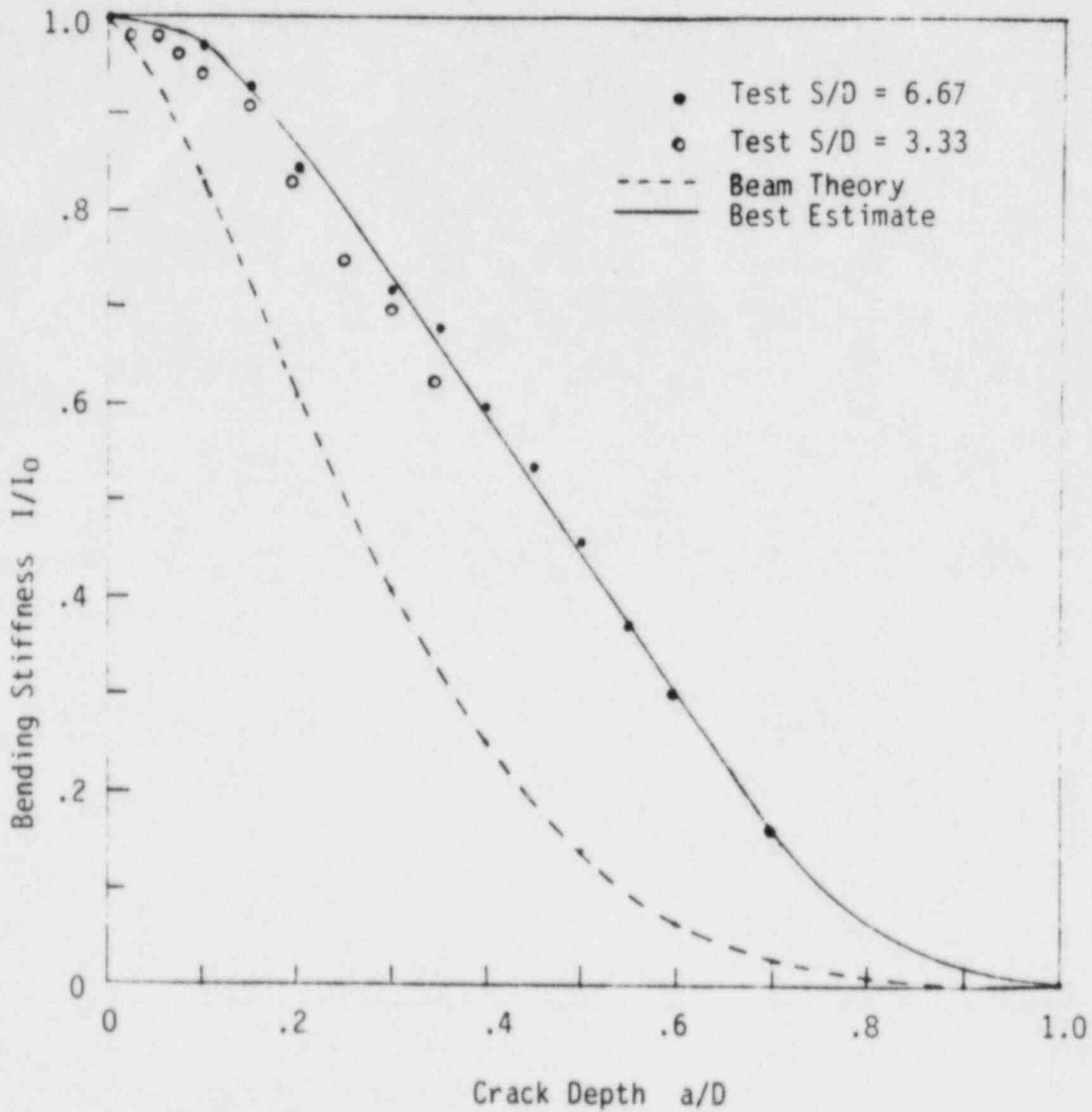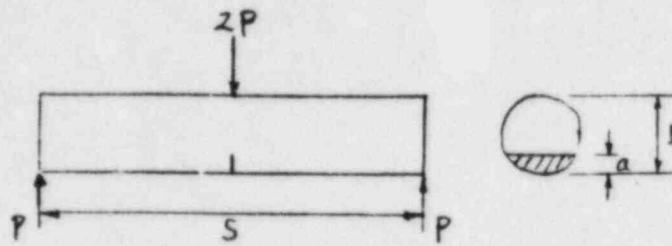
Beam Theory:

$$I_O = \frac{1}{4} \pi R^4$$

$$I = R^4 \left[\frac{1}{8} (2\alpha - \sin 2\alpha) \left(\frac{1 + 2 \sin^3\alpha \cos\alpha}{\alpha - \sin\alpha \cos\alpha} \right) - \frac{8}{9} \frac{\sin^6\alpha}{(2\alpha - \sin 2\alpha)} \right]$$

STRUCTURAL
INTEGRITY
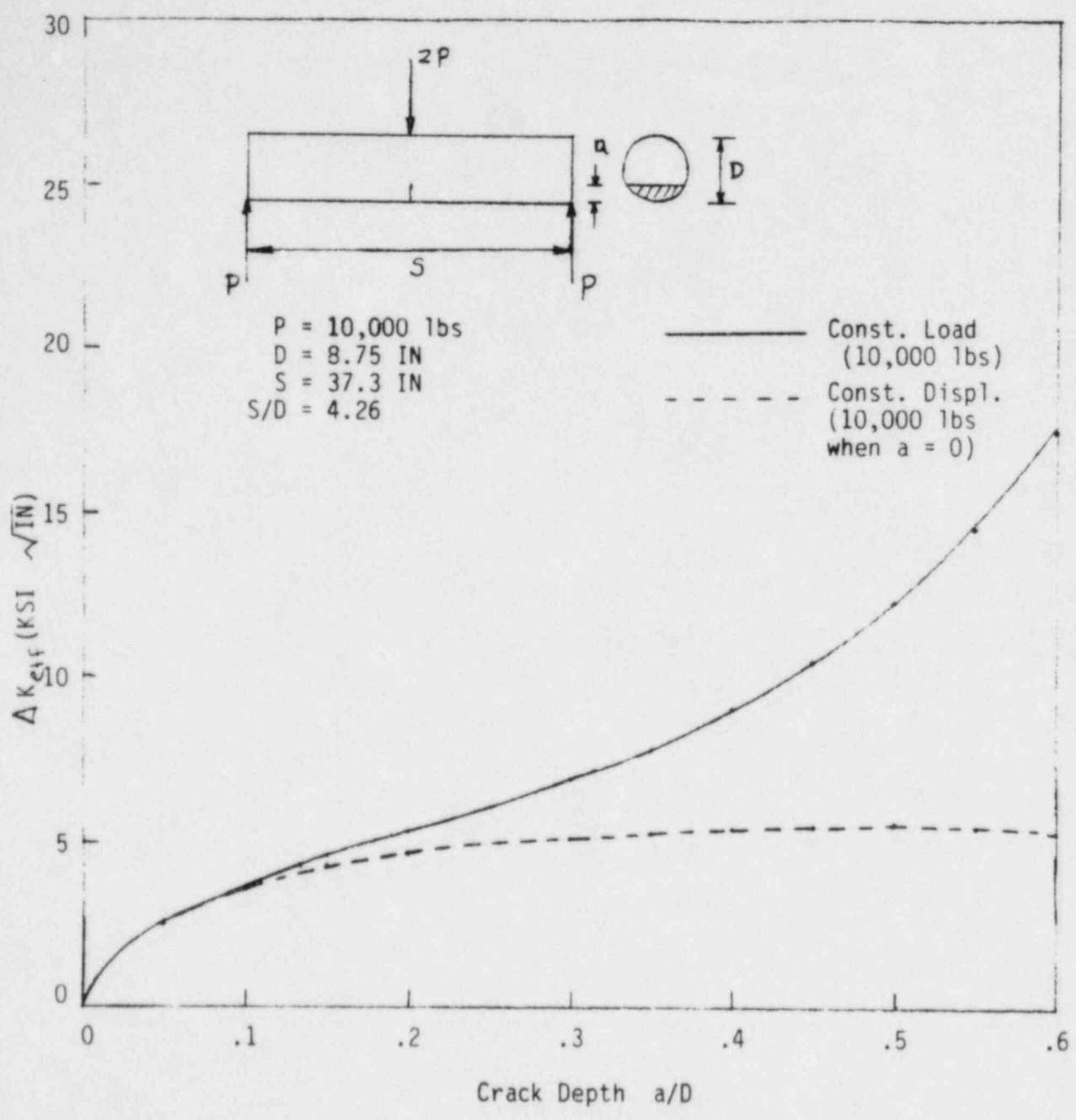
Figure 2-3 Stress Intensity Due to Radial Force = 10,000 Lbs. and
Constant Deflection
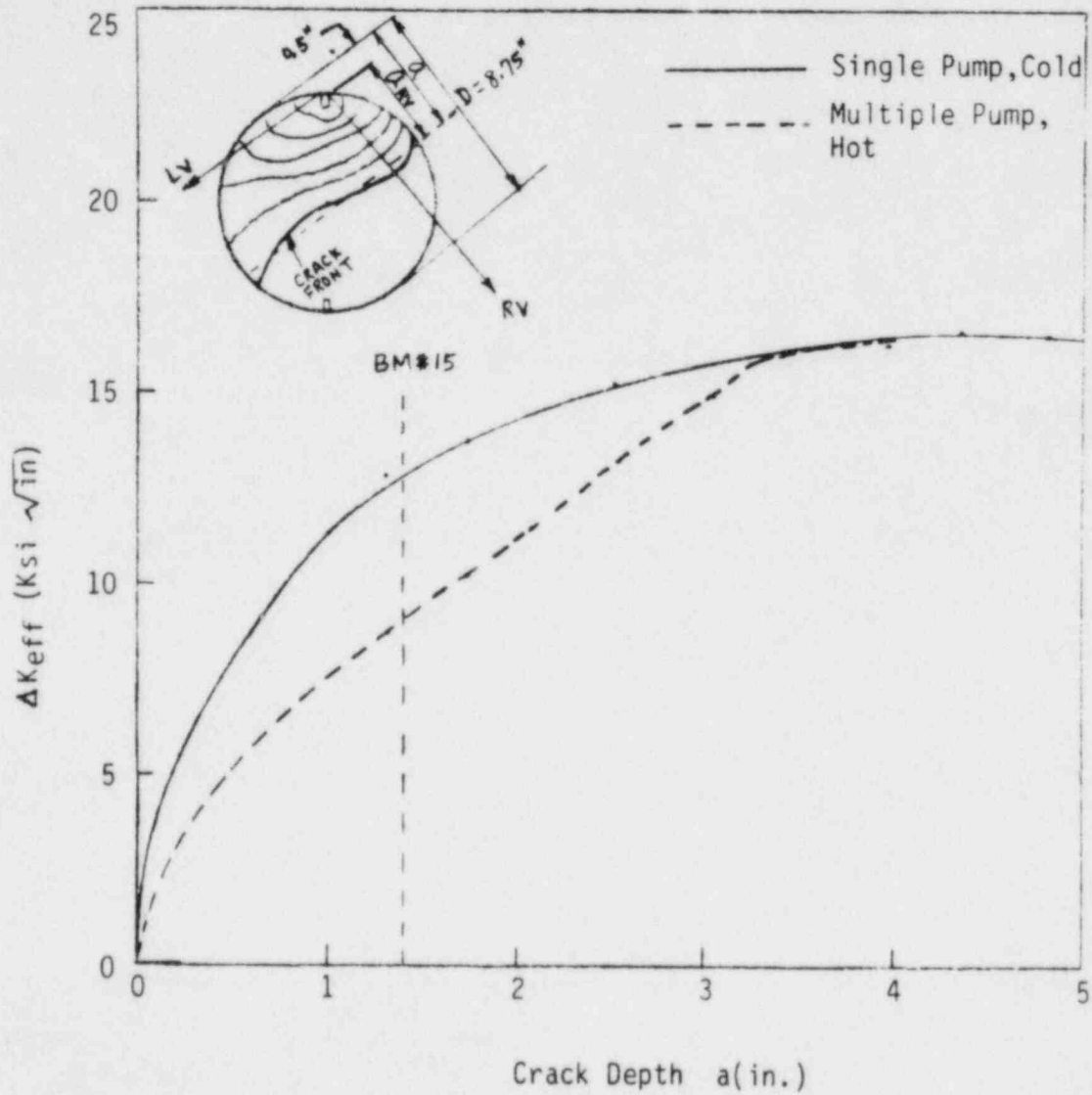
Figure 2-4 ΔK at Various Crack Depths (Due to Radial Thrust)

STRUCTURAL
INTEGRITY
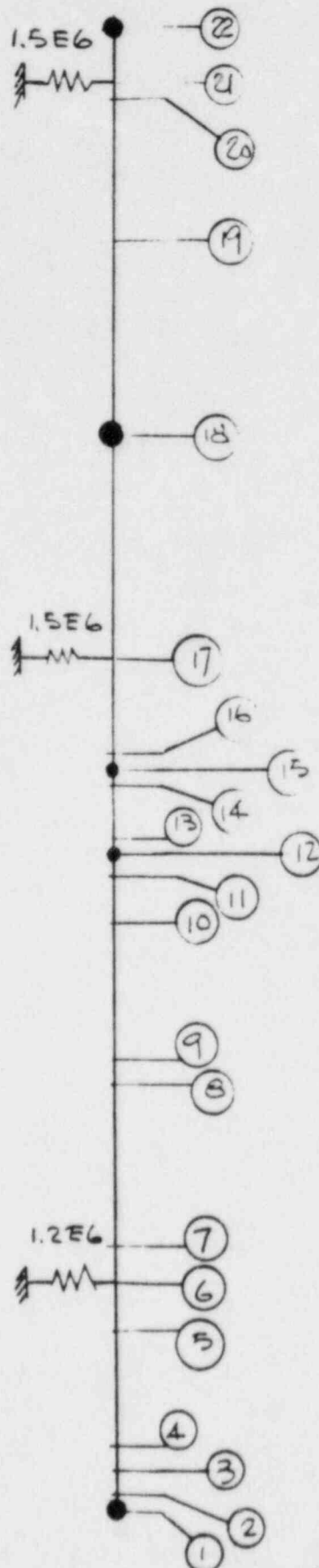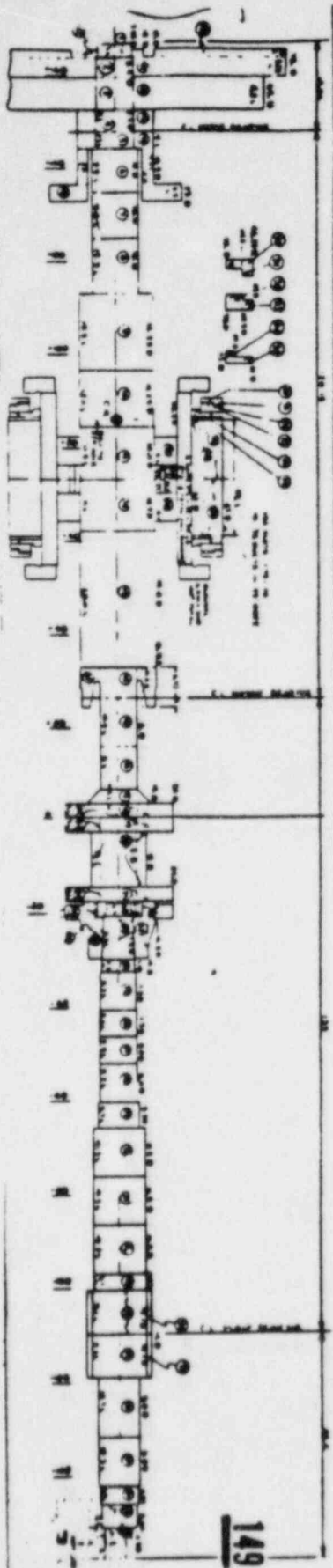
Figure 2-5 Finite Element Model
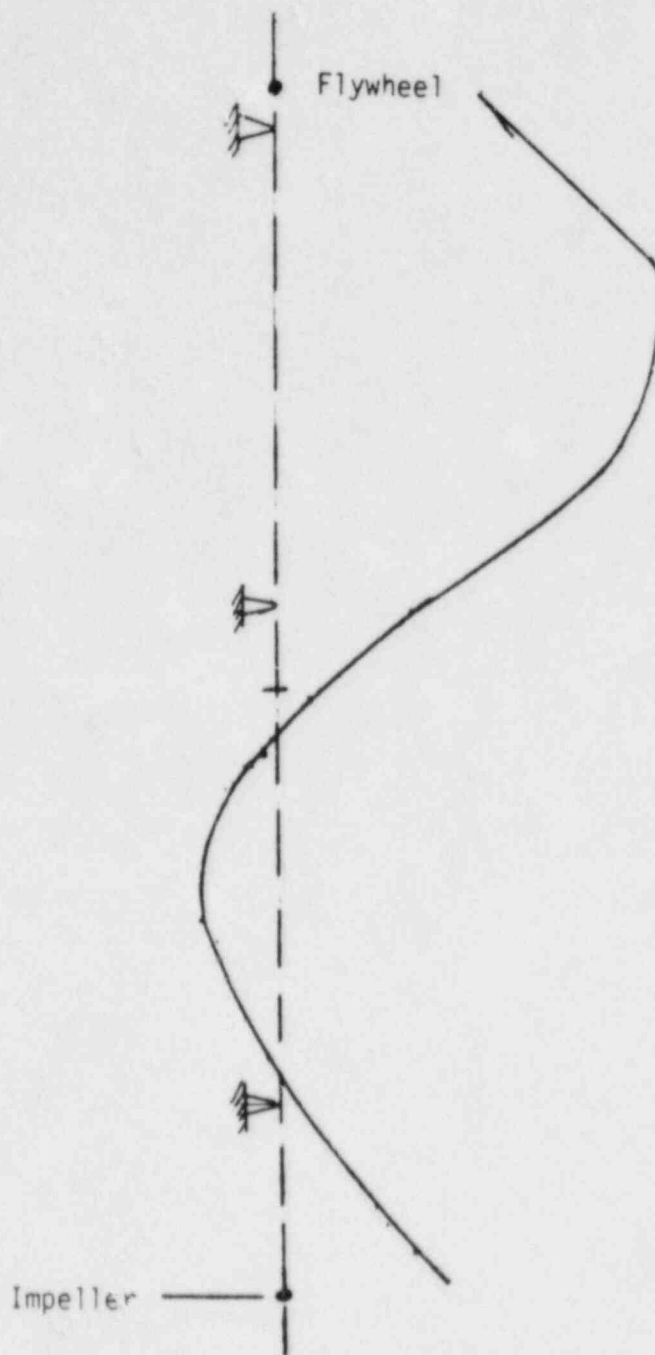
Figure 2-6 Bending Mode 1, Frequency = 26.3 Hz
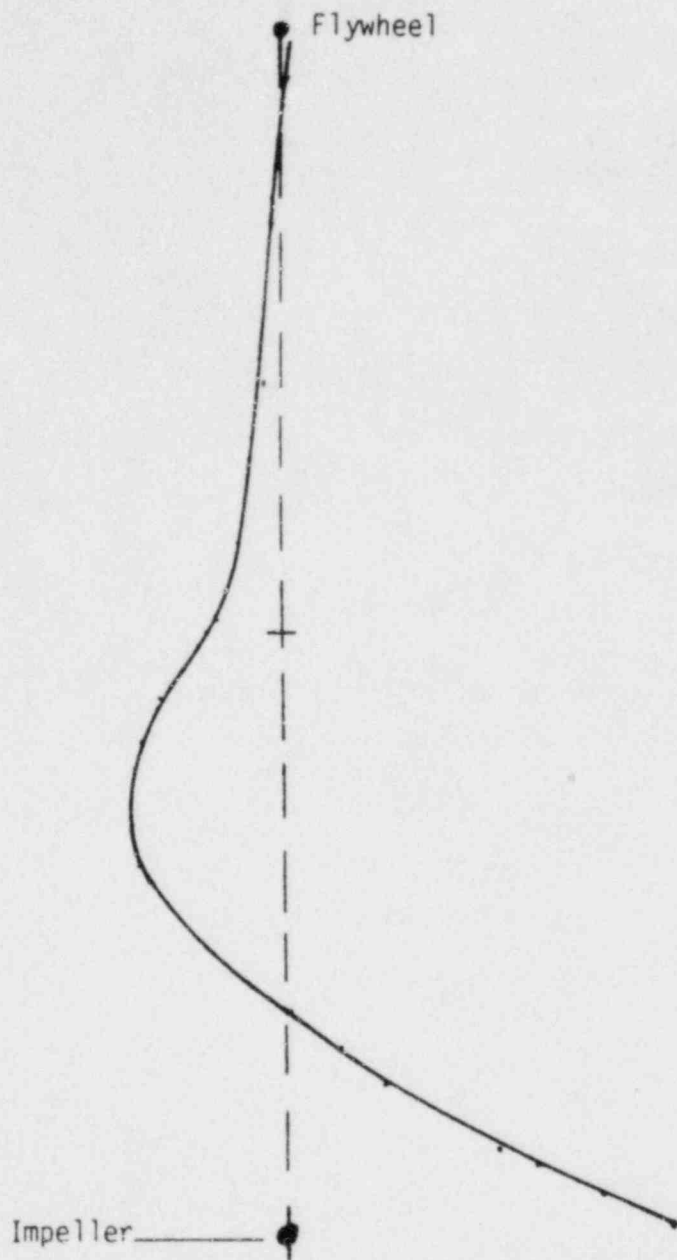
Figure 2-7 Bending Mode 2, Frequency = 27.26 Hz

STRUCTURAL
INTEGRITY
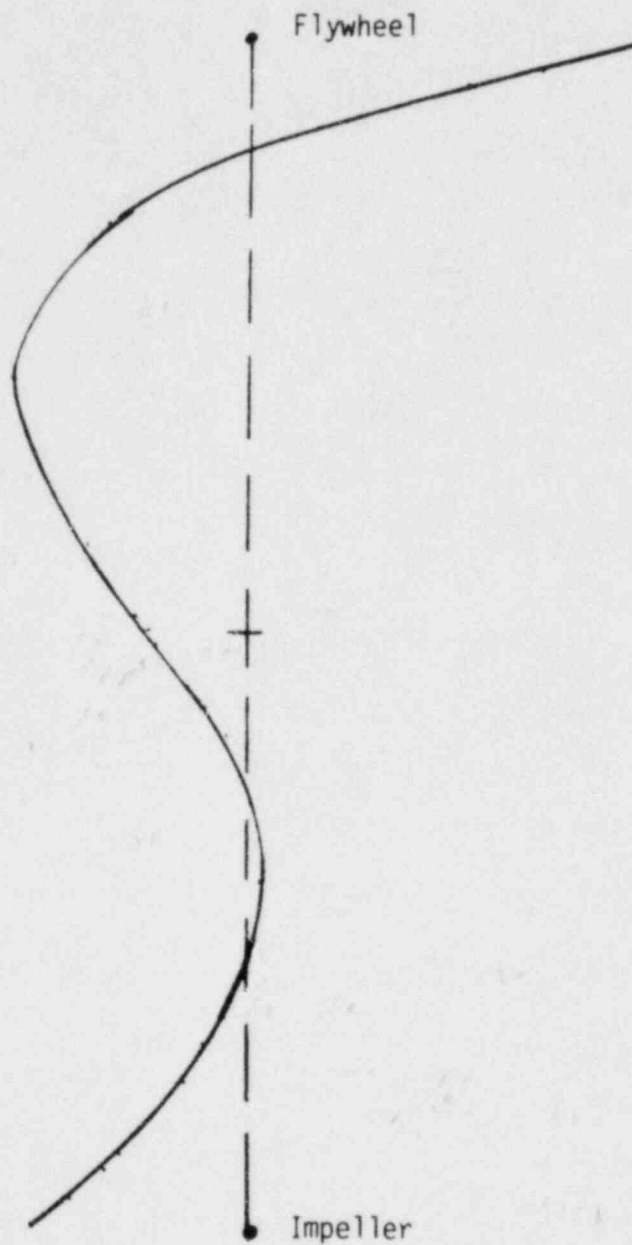
Figure 2-8 Bending Mode 3, Frequency = 31.98 Hz

Flywheel

Impeller
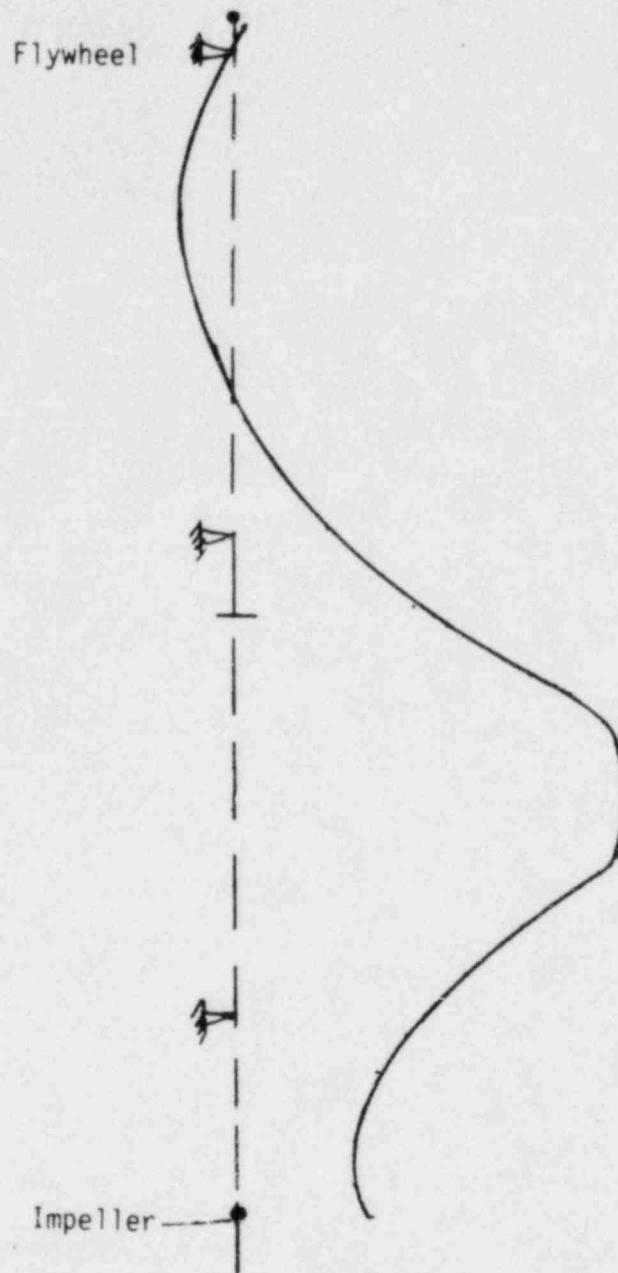
Figure 2-9   Bending Mode 4, Frequency = 50.84 Hz

STRUCTURAL
INTEGRITY
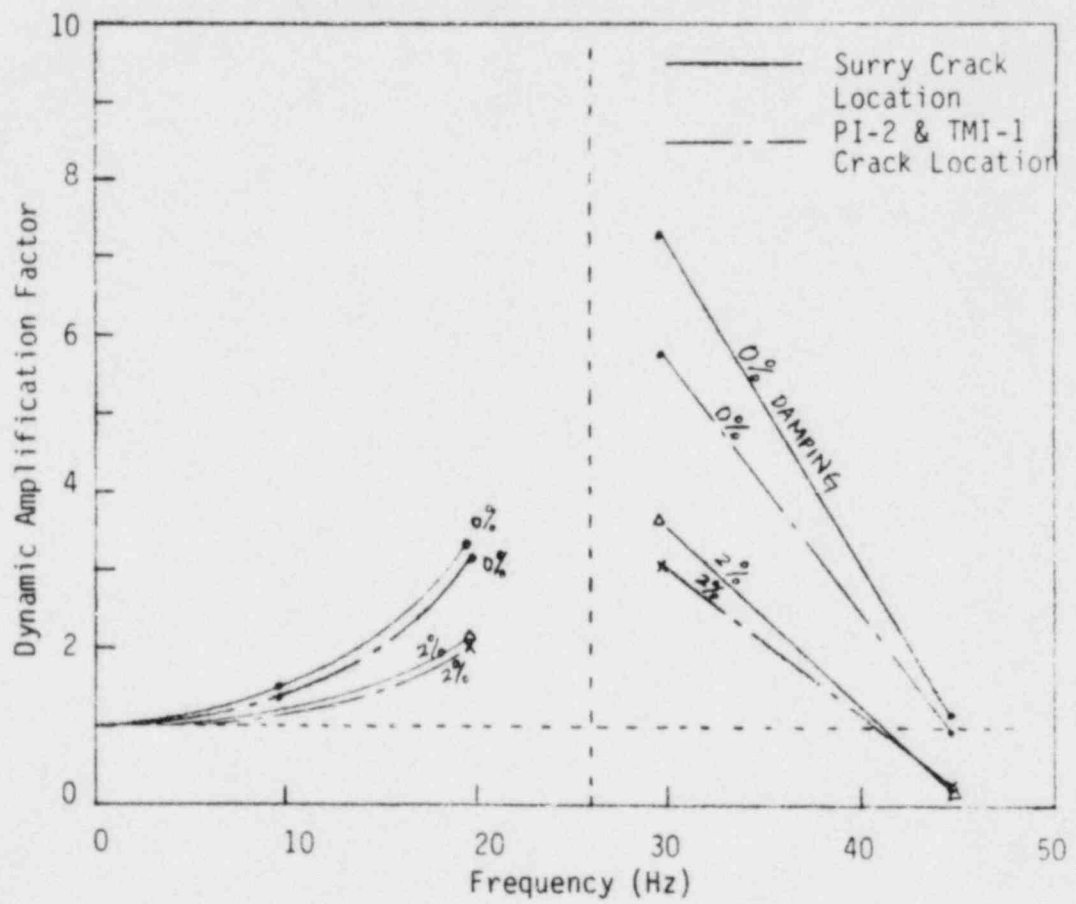
Figure 2-10 Dynamic Amplification Factors at the
Crack Locations

STRUCTURAL
INTEGRITY ASSOCIATES
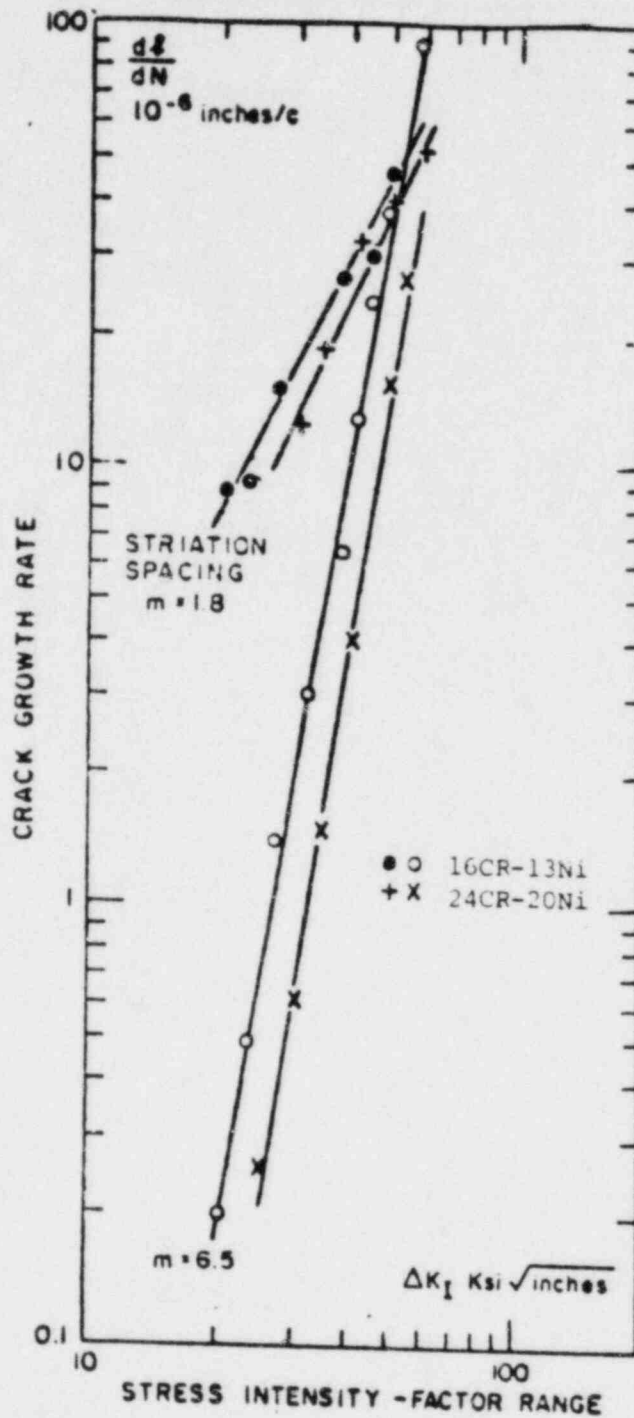
Figure 2-11 Macroscopic crack growth rates and striation spacing for two austenitic stainless steel. Tests conducted at room temperature, in air, at 10 Hz, with a constant minimum load. (From Bathius and Pelloux)
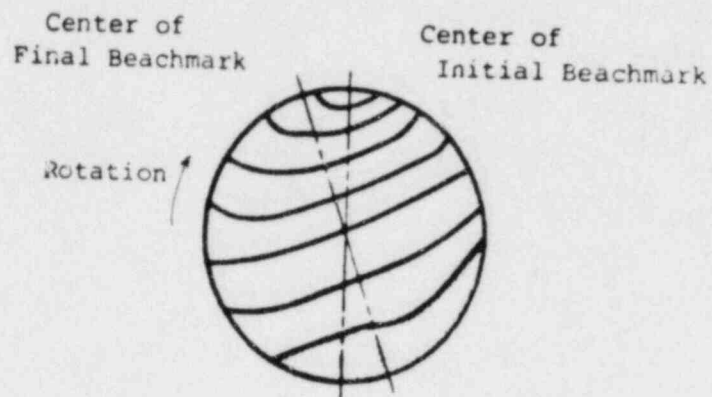
Figure 2-12 Example of Fracture Surface Indicating Unidirectional Bending with Low Bending Stress and Low Stress Concenration (From ASM Handbook, Vol. 10)
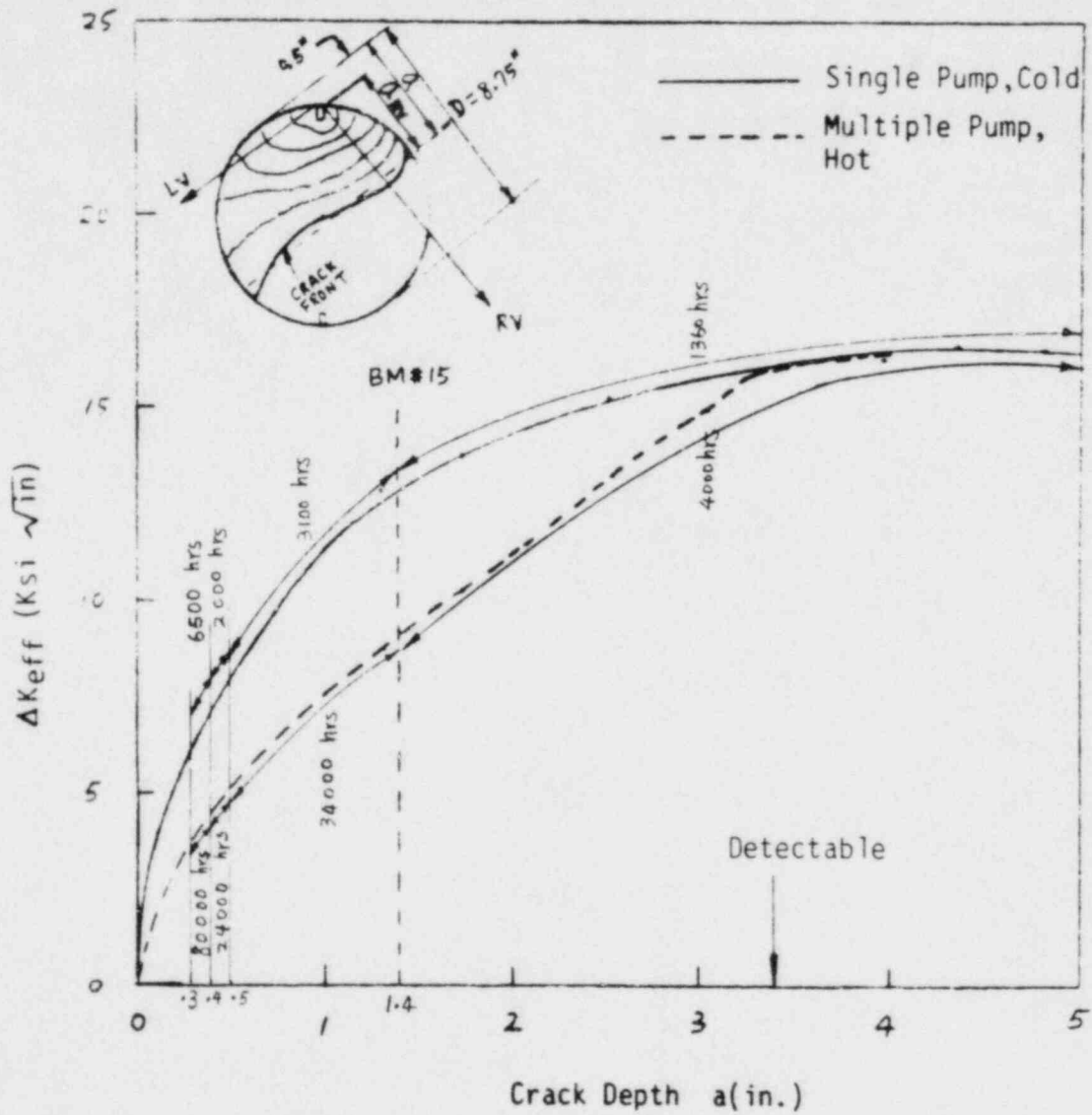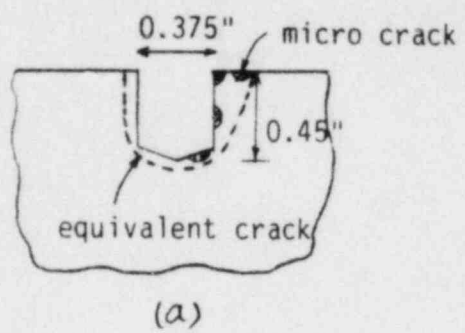
Figure 2-13 Fatigue Crack Growth of RCP Shafts

STRUCTURAL
INTEGRITY ASSOCIATES
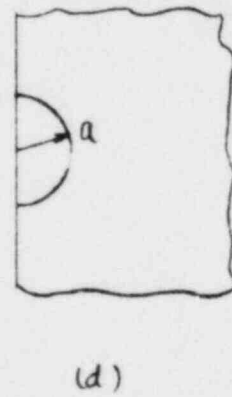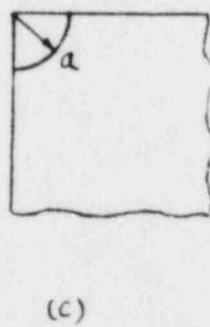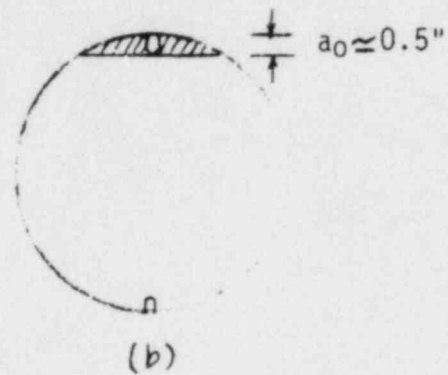
Figure 2-14 Micro-Crack Models

STRUCTURAL
INTEGRITY
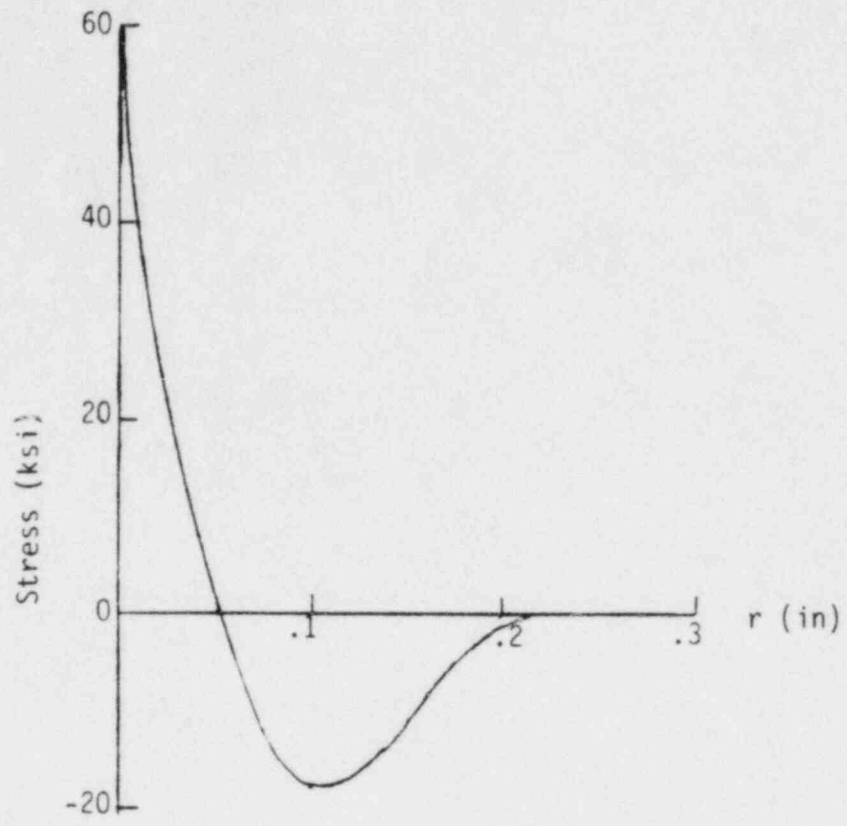
Figure 2-15 Assumed Residual Stress Distribution

STRUCTURAL
INTEGRITY ASSOCIATES
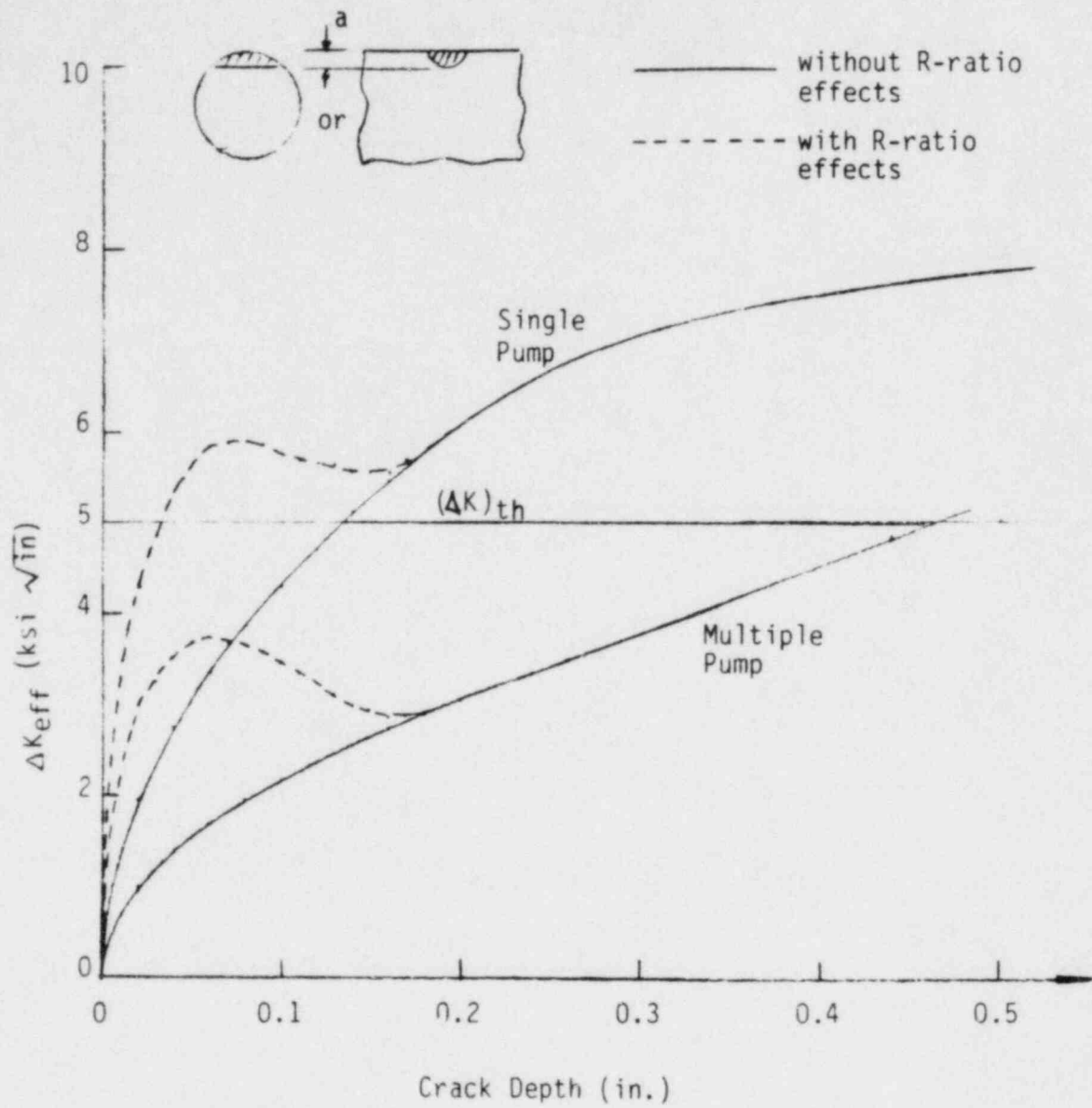
Figure 2-16 R-Ratio Effects Due to Residual Stresses

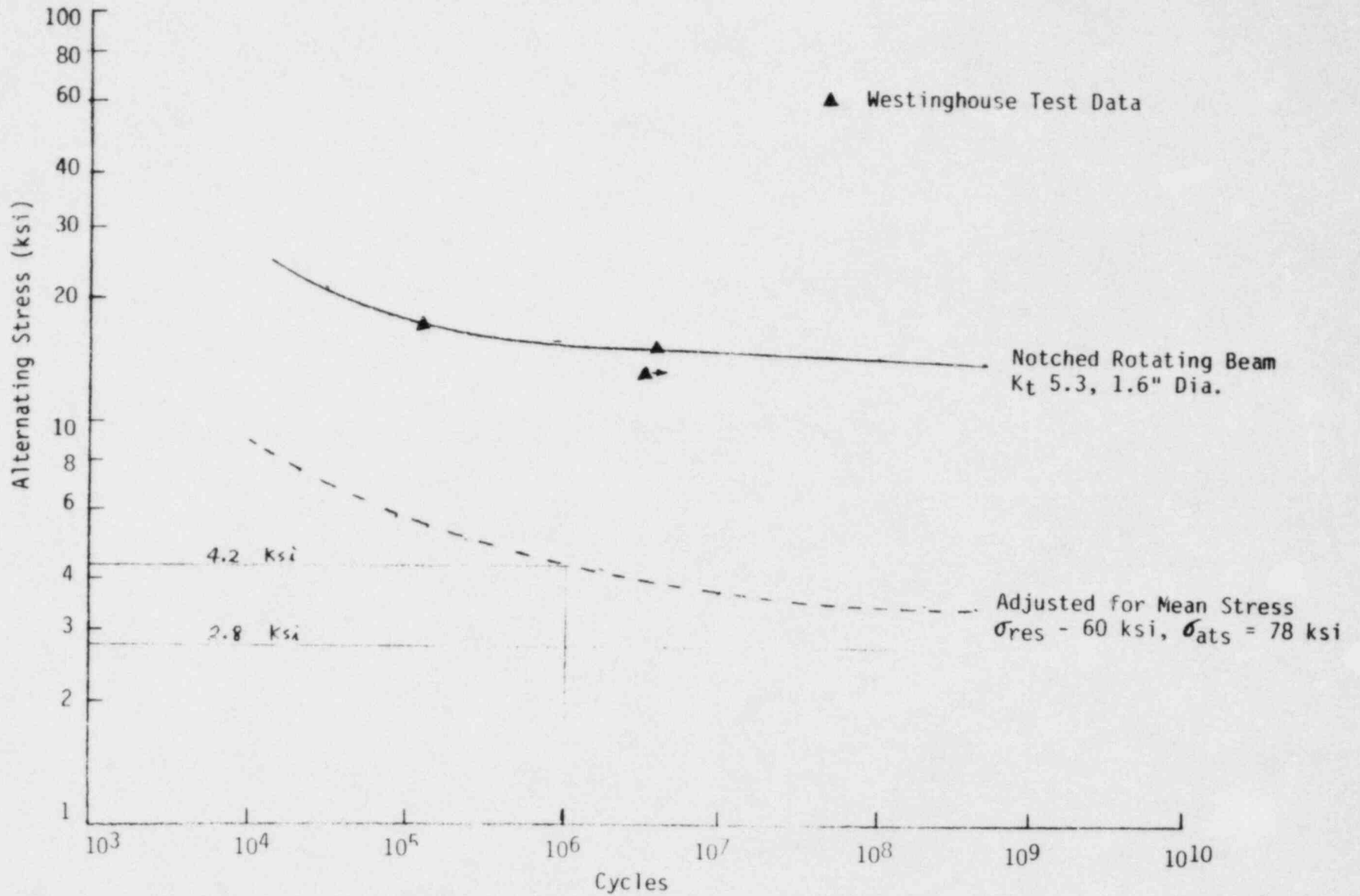STRUCTURAL
INTEGRITY associates

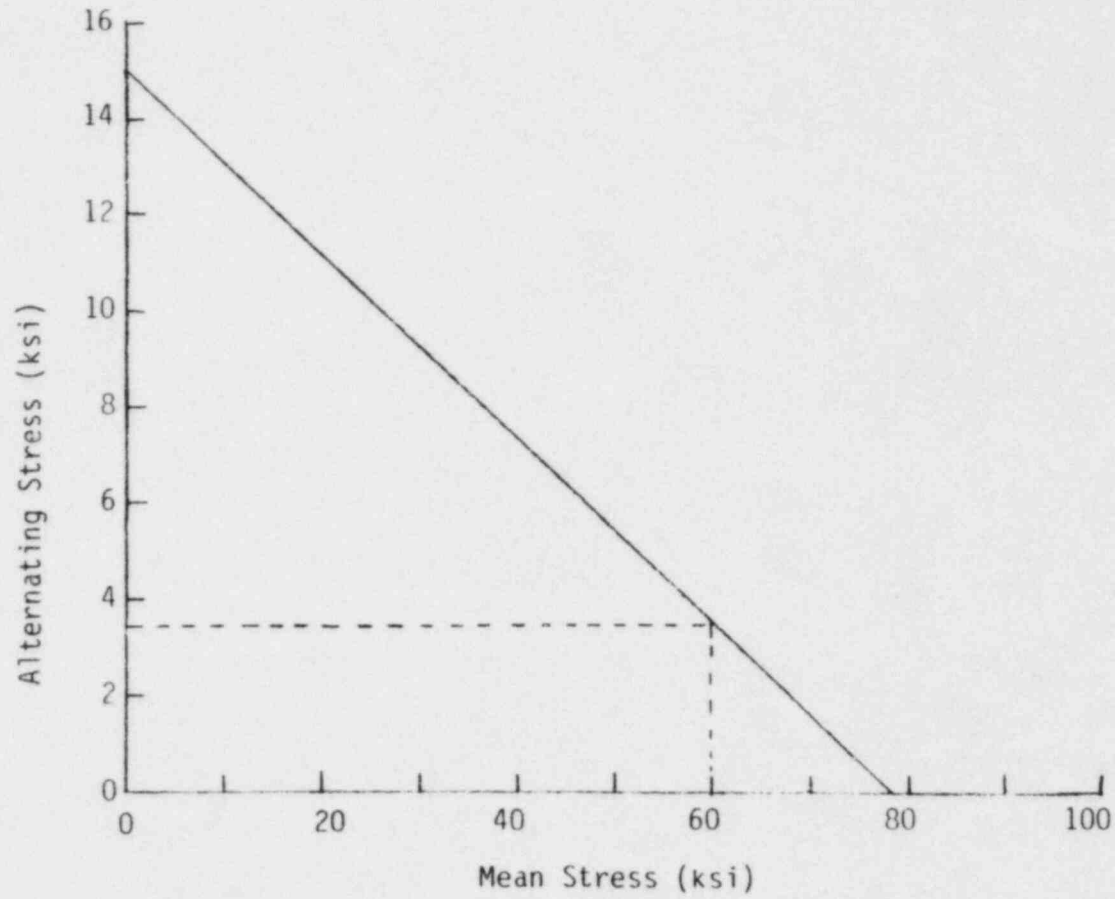Figure 2-17 Fatigue Tests of Type 347SS From Pump Shaft

Figure 2-18 Alternating Stress Required to Propagate a Small Crack 10^8 Cycle

3.0 Discussion/Conclusions

An analysis has been performed of crack initiation and growth in TMI-1 reactor coolant pump 1B. The analysis results are consistent with the observed failure conditions from the B&W metallurgical failure investigation, including striation spacing, observed beach marks on the fracture surface, and the observation that a 1.4 inch deep crack (BM #15) was present at the time of the 1979 shutdown.

Based on this analysis the following conclusions are drawn:

1. Considering worst case, yield level residual stresses from the pin welding operation, fatigue cracks can initiate in the shaft pin hole regions in approximately 10 hours of single pump operation.

2. Once initiated, the cracks can then propagate under either single or multiple pump operation. However, the propagation is considerably slower (~1 inch/30,000 hrs) under normal operation than under single pump operation (~1 inch/3,000 hrs), in the early stages of crack propagation.

3. Cyclic loading consistent with the observed failure is explanable due to radial thrust on the impeller, when one considers the potential for dynamic amplification at operating speed, plus the deflection restraints imposed by the clearances at the lower labyrinth seal.

4. Substantial crack depth on the order of 3.4 inches, is required before the failure can be detected by pump vibration monitors.

5. Based on conservative extrapolation of the pump B failure analysis, it is concluded that pump shafts A & C could also possibly contain incipient cracking on the order of 1.0 inches in depth, which would be subject to further propagation under either single pump or normal operational (multi-pump) loading.

6. The replacement shaft design in pump 1B is not believed to be significantly different than the original shafts from the standpoint of the above initiation and propagation mechanisms.

STRUCTURAL
INTEGRITY

4.0 References

1. B&W Preliminary Report, "TMI-1 Reactor Coolant Pump Shaft Failure Analysis", July 1984.

2. Unusual Safety Related Event Report No. USRE-S1-73-05, "Reactor Coolant Pump Shaft Failure", Surry Power Station, February, 1974.

3. Fickling, J. A., "Review of Model 93A Shafts in B&W Systems", Westinghouse Report, April 1974.

4. Riccardella, P. C., "Prairie Island, Unit 2, Reactor Coolant Pump Shaft Failure", Letter Report to Northern States Power Co. by N.TECH, October 1981.

5. Bush, A. J., "Experimental Determined Stress Intensity Factors for Single-Edge-Crack Round Bars Loading in Bending," Experimental Mechanics, pp. 249-258, July 1976.

6. STARDYNE User Information Manual, Mechanics Research, Inc., 1974.

7. Bathius, C., and Pelloux, R.M., "Fatigue Crack Propagation in Martensitic and Austenitic Steels", Metallurgical Transactions, Vol. 4, pp. 1265-1273, May 1973.

8. Bates, R. C., and Clark, W. G., Jr., Transaction Quarterly, The American Society of Metals, Vol. 02, p. 380, 1969.

9. American Society of Metals Handbook, Vol. 10, pp. 100-102.

STRUCTURAL
INTEGRITY